HHS Public Access

Author manuscript

J Control Release. Author manuscript; available in PMC 2021 August 10.

Published in final edited form as:

J Control Release. 2020 August 10; 324: 679–694. doi:10.1016/j.jconrel.2020.06.006.

Controlled Release of Odontogenic Exosomes from a Biodegradable Vehicle Mediates Dentinogenesis as a Novel Biomimetic Pulp Capping Therapy

W. Benton Swanson[1,+], **Ting Gong**[1,^,+], **Zhen Zhang**[1,&], **Miranda Eberle**[2], **David Niemann**[2], **Ruonan Dong**[1], **Kunal J. Rambhia**[4], **Peter X. Ma**[1,3,4,5,*]

[1]Department of Biologic and Materials Sciences, School of Dentistry, University of Michigan

[2]Department of Chemistry, College of Literature, Science, and the Arts, University of Michigan

[3]Macromolecular Science and Engineering Center, College of Engineering, University of Michigan

[4]Department of Biomedical Engineering, School of Medicine and College of Engineering, University of Michigan

[5]Department of Materials Science and Engineering, College of Engineering, University of Michigan

Abstract

Mineralized enamel and dentin provide protection to the dental pulp, which is vital tissue rich with cells, vasculature, and nerves in the inner tooth. Dental caries left untreated threaten exposure of the dental pulp, providing facile access for bacteria to cause severe infection both in the pulp and systemically. Dental materials which stimulate the formation of a protective dentin bridge after insult are necessary to seal the pulp chamber in an effort to maintain natural dentition and prevent pulpal infection. Dental materials to date including calcium hydroxide paste, mineral trioxide

[*]To whom correspondences should be addressed: Peter X. Ma, Ph.D., Richard H., Kingery Endowed Collegiate Professor, Department of Biologic and Materials Sciences, 1011 North University Ave., Room 2211, The University of Michigan, Ann Arbor, MI 48109-1078, Tel: (734) 764-2209, Fax: (734) 647-2110, mapx@umich.edu.

[^]Current Address: Hospital of Stomatology, Zunyi Medical University, Zunyi, 563000, China

[&]Current Address: Department of Orthopedic Surgery, West China Hospital, West China School of Medicine, Sichuan University, Chengdu, China

CRediT author statement

This work was carried out in the Polymeric Biomaterials and Tissue Engineering Laboratory at the University of Michigan. WBS and TG contributed overall equally to this work and drafted the manuscript. TG did mainly the biological and animal experiments including exosome isolation, cell culture, molecular and biochemical characterizations, subcutaneous implantation, pulp capping, and histological analysis. WBS did mainly the biomaterials and controlled release studies, including polymer synthesis, scaffold and microsphere fabrication, controlled release, and physical characterizations. ZZ, RD, and KJR participated in animal and biological studies. ME and DN participated in biomaterials and controlled release experiments. PXM organized and supervised the project, trained study participants, obtained funding, analyzed and interpreted data with trainees, revised and finalized the manuscript, and is the corresponding author.

[+]These two authors contributed equally to this work.

Supplementary Information

Supplementary Information is available at the website of *Journal of Controlled Release*.

Financial Disclosure

The authors have no competing financial disclosures or other conflicts of interest to report.

aggregate, and glass ionomer resin, are used with mixed results. Herein we exploited the cell-cell communicative properties of exosomes, extracellular vesicles derived from both mineralizing primary human dental pulp stem cells (hDPSCs) and an immortalized murine odontoblast cell line (MDPC-23), to catalyze the formation of a reactionary dentin bridge by recruiting endogenous stem cells of the dental pulp, through an easy-to-handle delivery vehicle which allows for their therapeutic controlled delivery at the pulp interface. Exosomes derived from both hDPSCs and MDPCs upregulated odontogenic gene expression and increased mineralization *in vitro*. We designed an amphiphilic synthetic polymeric vehicle from a triblock copolymer which encapsulates exosomes by polymeric self-assembly and maintains their biologic integrity throughout release up to 8–12 weeks. The controlled release of odontogenic exosomes resulted in a reparative dentin bridge formation, superior to glass-ionomer cement alone *in vivo*, in a rat molar pulpotomy model after six weeks. We have developed a platform for the encapsulation and controlled, tunable release of cell-derived exosomes, which maintains their advantageous physiologic properties reflective of the donor cells. This platform is used to modulate downstream recipient cells towards a designed dentinogenic trajectory *in vitro* and *in vivo*. Additionally, we have demonstrated the utility of an immortalized cell line to produce a high yield of exosomes with cross -species efficacy.

Graphical Abstract

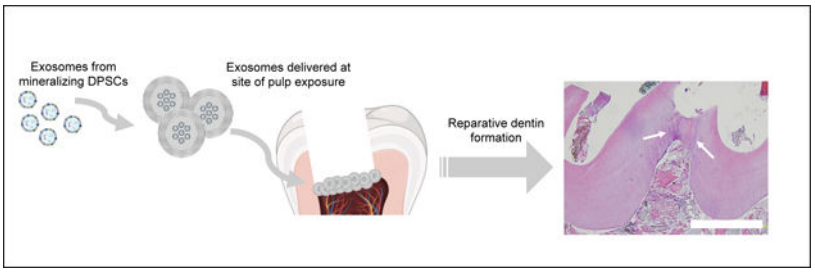

Keywords

Exosome; Controlled Release; Tissue Engineering; Pulpotomy; Dentin

Introduction

Nearly two and a half billion adults and five million children worldwide suffer from dental caries—the most common noncommunicable disease in the world [1, 2]. Severe tooth decay leads to obliteration of the pulp—the teeth's living tissue—and other comorbidities including periodontal disease and ultimately tooth loss. Caries left untreated provide a route of entry for bacteria into the body through the vasculature of the pulp. Direct and indirect pulp therapies induce tertiary mineralized dentin secretion to seal the vital pulp chamber from potential insult by the formation of a tertiary dentin bridge, a defensive reaction in the hard tissue of the tooth [3]. Tertiary dentin formation can be catalyzed or compensated for by dental materials [4]. The goal of these vital pulp therapies is to restore dynamic equilibrium to the dental pulp following exposure and mitigate potential for inflammatory response or loss of tooth vitality. Oral health is a key indicator of overall health, wellbeing,

and quality of life [5]. Therefore, safe and efficacious treatments to preserve dentition are important.

Most dental materials to date serve as substitutes to native tissue or encourage partial tissue formation around the material. Few are able to catalyze tissue neogenesis to restore original dentin integrity, providing complete defense to the pulp [6]. Dental pulp stem cells are a stem cell population that resides in the inner pulp chamber of teeth, proliferate rapidly, differentiate to secrete mineralized dentin, and are inducible by many known factors [7, 8]. Stem cell-based approaches to tissue engineering have been broadly explored in dental applications, including clinical studies. However, stem cell-based therapies, while efficacious, are expensive, difficult to commercially produce, and pose immunogenic concerns [9]. We hypothesized that a biologic which recapitulates the advantageous properties of stem cells, could modulate the phenotype of endogenous stem cells and guide their trajectories towards functional mineralized tissue regeneration *in situ*, when paired with an appropriate delivery platform, as an alternative to existing mineral-based cements. It is known that various biological factors are sequestered in natural tissue extracellular matrix (ECM) that can activate stem cells to initiate regeneration/repair programs, including regeneration of mineralized tissues such as bone and dentin [10–12]. It has also been reported that certain matrix metalloproteinases are able to digest dentin ECM and release matrix components to promote tertiary dentin formation [13]. Inspired by ECM, biomimetic nanofibrous scaffolds and growth factor release have been utilized to facilitate dentin and pulp tissue regeneration [14–16]. The biologic evaluation of new dental pulp capping materials should include consideration for pulp vitality, immune response and infection prevention, and the completeness of tertiary dentin bridge formation, in addition to traditional molecular biology approaches to gauging pro-mineralization potential.

Exosomes are lipid bi-layer bound vesicles produced through the multivesicular body pathway of exocytosis, sized 50–150 nm in diameter [17, 18]. Exosomes and extracellular vesicles are secreted by a variety of differentiated and stem cell types across physiologic systems, including DPSCs [19]. They are known to carry nucleotide and protein cargo, specifically microRNAs (miRNA) which can modulate the phenotype and activity of recipient cells as miRNA is transferred from the exosome to recipient cell cytoplasm by membrane fusion. The specific miRNA profile of exosome populations is a function of their donor cell identity and microenvironmental conditions. Therefore, the cargo is tunable based on strategic selection of cell source and culture conditions [20, 21]. The promising therapeutic potential of exosomes has been demonstrated across a number of diseases [22–24].

Exosomes from DPSCs have been shown to enhance mineralization and upregulation in characteristic odontogenic genes *in vitro* via activation of the MAPK pathway, partnered with immunogenic properties [25, 26]. Exosomes are also implicated in tooth development [27, 28]. A hinderance to their therapeutic use is a platform which allows for their easy handling and controlled local delivery. In the context of dentin tissue engineering, a single administration of a biomaterial is desired to facilitate healing over the course of weeks to months *in vivo*, while maintaining an isolated, sterile environment to prevent infection of the vital dental pulp as the dentin bridge forms.

Poly(lactic-co-glycolic acid) (PLGA) is a biodegradable polymer commonly used in FDA-approved drug delivery applications. It is a random copolymer with highly tunable properties; the relative hydrophilicity can be tuned by modulating the ratio of lactide (more hydrophobic) to glycolide (less hydrophobic) monomer to determine the rate of degradation and thus release profile of encapsulated cargo [29]. The double emulsion method is the most common method of cargo encapsulation by PLGA, demonstrated extensively with small molecules, protein growth factors, and plasmids [30, 31]. Sufficient stabilization of proteins and plasmids, for example, is required to preserve their integrity. In our efforts to encapsulate and deliver cell-derived exosomes locally, we hypothesized that the exosome lipid membrane must also be stabilized to protect its nucleotide cargo. Stabilization may be accomplished through external stabilizing agents added to the double emulsion, as a property of the polymer's chemistry, or a combination of these two methods [32]. PLGA spheres can be administered efficiently as injectable suspensions or pastes; their poly(aliphatic ester) backbone degrades by hydrolysis on contact with water to release cargo. PLGA spheres have been used in the controlled release of small molecules for dental tissue engineering therapies previously, including at the pulp interface, demonstrating their safety [33, 34].

We propose an alternative to mineral cements as a pulp capping material, which relies on PLGA-based biodegradable microspheres for the sustained elution of pro-dentinogenic exosomes derived from either primary cells or cell-lines following pulp exposure. We aim to induce the migration and differentiation of resident DPSCs in the pulp to regenerate new mineralized reactionary dentin at the insult site, on a clinically relevant time scale. In this study we use a self-assembling synthetic PLGA based triblock copolymer vehicle with tunable degradation properties to encapsulate and controlled release dentinogenic exosomes, and evaluate their potential as a regenerative pulp capping biomaterial using in vitro and in vivo models.

Materials and Methods

Materials:

Polyethylene glycol (PEG, M_w = 1,000 g/mol, 2,000 g/mol, 6,000 g/mol), methyl-polyethylene glycol (M_W = 1,000 g/mol), α-bromoisobutyryl bromide (BIBB), polyvinyl alcohol (PVA) (Aldrich); L-lactide (Altasorb); glycolide, stannous octanoate ($Sn(Oct)_2$), 2-hydroxyethyl methacrylate (HEMA), azobisisobutyronitrile (AIBN), triethylamine (TEA), copper (I) bromide (CuBr), dissodium hydrogenphosphate (Na_2HPO_3), N,N,N′,N″,N″-pentamethyldiethylenetriamine (PMDETA), Span® 80, alkaline phosphatase staining kit, collagenase type I, ascorbic acid, β-glycerophosphate, dexamethasone (Sigma); nile blue acrylamide (Polysciences); tetrahydrofuran (THF), diethyl ether, 9-anthracecenylmethyl methacrylate, hexane, methanol, methylene chloride, isopropanol, TRIzol, micro BCA protein assay kit, Alexa-Fluor 555 phalloidin, ProLong Gold Anti-Fade, Alizarin Red S staining solution, conjugated secondary antibody, sodium dodecyl sulfate (Fisher Scientific); D-Trehalose, D-fructose (Oakwood Chemical); mineral oil (Alfa Aesar); deuterated NMR solvents ($CDCl_3$, D_2O) (Acros Organics); chloroform (VWR Chemical); ethanol (Decon Labs); dialysis tubing (3,500 M_W cutoff) (Spectrum Labs); Electron-microscopy grade

paraformaldehyde (EMS Diasum); Dulbecco's Modified Eagle Medium, fetal bovine serum (FBS), exosome-depleted FBS, penicillin, streptomycin, phosphate buffered saline (PBS), ascorbic acid, dexamethasone (Gibco); All-In-One RT MasterMix (Applied Biological Materials Inc.); 7500 Real Time PCR System, PowerUp Sybr Green Master Mix (Applied Biosystems); EpiQuik Whole Cell Extraction Kit (Epigentek); 4–12% Bis-Tris gels (NuPAGE); PVDF membrane (BioRad); BrightStar ECL detection kit (Alkali Scientific); Formvar-carbon coated electron microscopy grid (Ted Pella); miRNeasy Mini Kit (Qiagen). Molar defects were made with a diamond bur (*6878K series*, Nobel Biocare, Sweden) and hand-filed with an endodontic K-file (size 15, Kerr). Defects were sealed with glass ionomer GC Fuji IX GP 1–1 (GC Corporation).

Diblock and Triblock PEG and PLGA Copolymer Synthesis:

We designed two copolymers: triblock PLGA-PEG-PLGA, and diblock PEG-PLGA, which were synthesized from HO-PEG-OH and H_3C-PEG-OH initiators, respectively. In a round bottom flask, stoichiometric amounts of L-lactide and glycolide monomers, PEG, and $SnOct_2$ catalyst (monomer/$Sn(Oct)_2$ = 100) were combined. The system was held under positive nitrogen pressure for 30 minutes, and heated to 120°C, where the reaction proceeded by stannous-catalyzed ring opening polymerization for 120 minutes under inert conditions. Polymers are abbreviated as PL_XG_YA-PEG-PL_XG_YA where X and Y represent percentages of lactide and glycolide. A typical procedure is as follows ($PL_{70}G_{30}$-PEG-$PL_{70}G_{30}A$): 1.25g HO-PEG-OH (M_W=1,000 g/mol), 3.00 g L-lactide, 2.00 g glycolide and 112 uL $Sn(Oct)_2$ were added to a round bottom flask with stirring and nitrogen purging for 30 minutes, then heated to 120°C to melt, and the reaction was carried out for 120 minutes as the molten reaction mixture became solid. The crude product was dissolved in a minimum amount of chloroform, precipitated into 5-times excess volume of cold methanol, and collected by vacuum filtration, twice to purify. ^{1}H NMR (400 MHz, $CDCl_3$): δ 1.5 ppm, s, sp^3 CH_3; 3.6 ppm, m, sp^3 CH_2; 4.8 ppm, m, glycolide sp^3 CH_2; 5.2 ppm, m, lactide sp^3 CH.

Fluorescent Polymer Synthesis:

Following methods developed by our group [35], fluorophores were used to label end-groups of polymer blocks in the block copolymers described above to probe at their self-assembling nature in exosome-containing microsphere (EXO-MS) fabrication. The details are described in the following 3 subsections.

Synthesis of HEMA-PLLA: Acrylic-end functionalized PLLA was synthesized from (hydroxyethyl)methacrylate (HEMA) initiator (0.8 mmol, 86 μL) and L-lactide monomer (40 mmol, 5.760 g), catalyzed by $Sn(Oct)_2$ (112 μL) in a ring opening polymerization at 120°C, in an inert N_2 environment [36, 37]. At completion, the polymer was dissolved in 20 mL chloroform, and precipitated in 100 mL cold methanol (5x volume), where the product was collected by vacuum filtration, twice to remove unpolymerized monomer. ^{1}H NMR (400 MHz, $CDCl_3$): δ 1.6 ppm, s, sp^3 CH_3; 5.1 ppm, q, sp^3 CH; 5.8 ppm, dt, sp^2 CH; 6.1 ppm, dd, sp^2 CH; 6.4 ppm, dd, sp^2 CH.

Synthesis of Nile Blue-PLLA: HEMA-PLLA (1.40 g), nile blue acrylamide (0.012 mmol, 0.005 g), and freshly recrystallized azobisisobutyronitrile (AIBN, 0.06 mmol, 0.0098

g) were dissolved in 10 mL dioxane; the reaction was heated to 70°C where it was allowed to proceed for 24 hours. Solvent was removed by rotary evaporation, the product was redissolved in a minimum amount of $CHCl_3$ and precipitated into cold methanol, then collected by suction filtration. This purification step was repeated approximately four times, until the methanol is no longer visibly colored by unreacted dye. ^{1}H NMR (400 MHz, $CDCl_3$): δ 1.5 ppm, s, sp^3 CH_3; 5.1 ppm, q, sp^3 CH; 7.5–8.5 ppm, m, sp^2 CH.

9-Anthracenylmethyl methacrylate-PEG: Br-PEG-OH was synthesized from HO-PEG-OH (10 g, M_w = 1,000 g/mol) dissolved with triethylamine (TEA, 2.2 mL) in anhydrous tetrahydrofuran (THF, 50 mL) and purged under nitrogen for 30 minutes. The reaction was submerged in an ice bath and α-Bromoisobutyryl bromide (BIBB, 1.2 mL) was added dropwise with a syringe over the course of one hour. The solution stirred for 24 hours and warmed to room temperature gradually as the ice melted. After 24 hours, solvent was removed by rotary evaporation. The residue was redissolved in a minimum amount of dichloromethane (DCM), precipitated into cold diethyl ether (5x excess volume), and collected by vacuum filtration, twice. The resulting Br-PEG-OH was frozen at −80°C and lyophilized for 48 hours to remove residual water. ^{1}H NMR (400 MHz, D_2O): δ 3.07 ppm, q, -CH_2-Br; 3.5–3.6 ppm, m, -CH_2CH_2O-.

To make Br-PEG-PLLA, Br-PEG-OH (1.24 g) was mixed with L-lactide (5 g) and $Sn(Oct)_2$ (112 μL) in a round bottom flask, purged with nitrogen for 30 minutes, with stirring. After 30 minutes, the mixture was heated to 120°C for 120 minutes, to carry out ring opening polymerization in bulk. At completion, the residue was redissolved in a minimum amount of $CHCl_3$, precipitated into cold methanol (5x excess), and collected by vacuum filtration twice. ^{1}H NMR (400 MHz, $CDCl_3$): δ 1.56 ppm, sp^3 CH_3; 3.1 ppm, q, -CH_2-Br; 3.6–3.65 ppm, m, -CH_2CH_2O-; 4.7–4.8 ppm, m, glycolide sp^3 CH_2; 5.1–5.2 ppm, m, lactide, sp^3 CH.

9-anthracecenylmethyl methacrylate was polymerized from the terminal bromide via atom transfer radical polymerization (ATRP). Br-PEG-PLLA (2 g), 9-anthracenylmethyl methacrylate (0.1 g), and CuBr (0.04 g) was added to a round bottom flak and purged with nitrogen for 40 minutes. Separately PMDETA (200 μL) was dissolved in deionized H_2O (40 mL), also purged with nitrogen. After 40 minutes, the PMDETA-water solution was added via a syringe to the round bottom flask containing the polymer and stirred for 24 hours at room temperature. The resulting solution was dialyzed against deionized water using 3,500 M_w cutoff dialysis tubing, changing the water daily for three days, then the solution was frozen to −80°C and lyophilized. ^{1}H NMR (400 MHz, $CDCl_3$): δ 1.56 ppm, sp^3 CH_3; 3.6–3.65 ppm, m, -CH_2CH_2O-; 4.7–4.8 ppm, m, glycolide sp^3 CH_2; 5.1–5.2 ppm, m, lactide, sp^3 CH, 5.6 ppm, d, sp^3 CH_2; 6.1–6.2 ppm, m, sp^2 CH; 6.5, d, sp^2 CH; 7.5–7.7 ppm, dq, sp^2 CH_2; 8.2 ppm, d, sp^2 CH.

Gel Permeation Chromatography:

Polymer samples were dissolved in THF at a concentration of 5 mg/mL and filtered using a 200-μm syringe filter. The GPC analysis was performed on a Shimadzu GPC system containing three columns in series with a refractive index detector and a diode array UV-Vis

detector. The GPC was calibrated with narrow polydispersity polystyrene standards and the molecular weights are reported as polystyrene equivalents.

Nuclear Magnetic Spectroscopy:

^1H spectra of the polymers were recorded with an Inova 400 NMR instrument (Varian), operating at 400 MHz at room temperature, using $CDCl_3$ or D_2O as solvent.

Exosome Containing Microsphere (EXO-MS) Fabrication:

PEG-PLGA copolymer (diblock or triblock) microspheres containing exosomes were fabricated using a mechanical water-in-oil-in-water (w/o/w) double emulsion method. Exosomes were concentrated to at least 2,000 μg/mL in PBS, to which D-Trehalose was added stoichiometrically to make a 2 mM solution. PEG-PLGA copolymer was dissolved in dichloromethane (DCM, 5% w/v). 300 μL of the exosome-trehalose solution was aliquoted into 2 mL of the PEG-PLGA/DCM solution and stirred quickly for 10 minutes to cause an emulsion (Level 10, Corning Magnetic Stir Plate). The primary w/o emulsion was emulsified into 20 mL polyvinyl alcohol (PVA, 1% w/v) solution to form the w/o/w double emulsion, under mechanical stirring (Level 8, Corning Magnetic Stir Plate). The resulting w/o/w double emulsion was left to stir at room temperature in a fume hood for 12 hours to evaporate the organic solvent, leaving behind solid polymer spheres which contained exosomes, dispersed in water. To slow the rate of evaporation, the w/o/w emulsion vessel was covered with foil with a few small holes. EXO-MS were collected by centrifugation (3,500 g, 8 minutes) and washed four times with fresh deionized water, then frozen and lyophilized. An exosome encapsulation efficiency of approximately 80% was achieved in the biodegradable PLGA-PEG-PLGA microspheres, which varied slightly with the polymer composition though. Morphology and size were evaluated as described below.

Polymer Particle Size Characterization:

The size of polymer spheres was determined by laser diffraction using a particle analyzer, carried out using a Malvern Mastersizer 2000 with Hydro 2000S wet dispersion unit. Samples were prepared in a suspension in deionized water (5 mg/mL) and added to the sample reservoir with stirring and sonication. Measurements assumed a default refractive index of 1.590 and solvent refractive index of 1.330.

SEM Characterization:

Particles were drop-cast onto carbon tape fixed to a specimen mount. Samples were sputtercoated with gold for 120 s (DeskII, Denton Vacuum, Inc.) and observed under a scanning electron microscope (Philips XL30 FEG) at 10 kV. Released exosomes, fixed in EM-grade PFA (10 %) overnight, were drop-cast onto carbon tape and coated for 90 s, observed at 5 kV.

Cell Isolation and Culture Conditions:

Fresh pulp tissue from sound human third molars (< 24 years old; n = 4, University of Michigan School of Dentistry Oral Surgery Clinic) was collected and subjected to enzymatic digestion by collagenase type 1 (3 mg/mL; Sigma-Aldrich). The resulting cells were re-

suspended in complete α-MEM (Minimum Essential Medium Eagle Alpha, supplemented with 10% fetal bovine serum (FBS), L- glutamine and 1% penicillin-streptomycin; GIBCO), and incubated for 3 hours in culture plates at 37°C and 5% CO_2 in a humidified environment. The adherent cells were then cultured in complete α-MEM. Cells at passage 3 to 6 were used in this study. Cell isolation from human specimens was in accordance with a protocol approved by the Institutional Review Board at the University of Michigan. MDPC-23 cells were a gift from Dr. Helena Ritchie (Department of Cariology, Restorative Sciences, and Endodontics, School of Dentistry, University of Michigan). MDPC-23 were maintained in Dulbecco's Modified Eagle's Medium (DMEM) containing 4.5 g/L glucose, 10% fetal bovine serum, and supplemented with an antibiotic solution (100 U/mL penicillin-G and 100 ug/mL streptomycin) at 37°C in a humidified atmosphere (5% CO_2). Primary DPSCs were isolated from mice for subcutaneous implantation experiments; maxillary and mandibular first molars were extracted from 6–8-week-old male mice and extracted in the same way as human DPSCs.

Isolation of Exosomes:

Cells were seeded to confluence in 100-mm cell culture dishes and cultured in odontogenic differentiation media (containing 50 μg/mL ascorbic acid, 5 mM β-glycerophosphate, and 10 nM dexamethasone; Sigma-Aldrich) for a period of 2 weeks. The status of mineralization was confirmed by Alizarin Red. Exosomes were isolated by differential centrifugation as previously published [38]. Briefly, one day prior to isolation, the cell cultures were washed in serum free odontogenic media and cultured for 24 hours. The conditioned media (CM) was centrifuged at 300×g for 10 minutes and 2000×g for 10 minutes to remove dead cells and debris. Then the supernatant was filtered through a 0.22-μm filter (GVS North America) to remove residual debris. The supernatant was centrifuged at 4000×g to about 200 μL in a 15 mL Amicon Ultra-15 Centrifugal Filter Unit (Millipore) for 10 minutes. The ultra-filtrated liquid was washed twice and centrifuged at 100,000×g for 70 minutes. Then the pellet was re-suspended and centrifuged at 100,000×g for another 70 minutes. The pellet was re-suspended with 200 μL phosphate buffered saline (PBS) and stored at −80°C until use. Exosomes were measured for their protein content, as a measure of sample concentration, using a BCA Protein Assay Kit (Pierce).

Fluorescent Labelling and Cellular Uptake of Exosomes:

Exosomes were labeled by carbocyanine dye DiO (Thermo Fisher Scientific) following a previously reported protocol [39]. Briefly, 10 μg/mL exosomes were incubated with DiO for 20 min at 37°C followed by PBS washing three times. 50,000 DPSCs were seeded on glass cover slides and cultured in 24-well-plates. Labeled exosomes were added to the culture media of cells and incubated for 30 minutes. Cells were washed with PBS and fixed with 4% paraformaldehyde (PFA). Immunofluorescence and confocal microscopy are described in detail below. To evaluate the uptake of exosomes released from EXO-MS polymer spheres, DiO labelled exosomes were used in the fabrication of EXO-MS, following the described particle fabrication protocol presented herein. Following lyophilization and sterilization, particles were incubated in PBS for two weeks, changing PBS every 48 hours, then with cell culture media for two hours on a shaker at 37°C. Particles were allowed to settle to the bottom of a 15-mL conical tube (Falcon), and supernatant conditioned media, containing

released fluorescently labelled exosomes, was collected and incubated with cells in the same method described above, for 30 minutes. Their uptake is visualized by confocal microscopy.

Western Blot for Exosome Surface Markers:

Total protein of exosomes was extracted with the EpiQuik Whole Cell Extraction Kit (Epigentek, Farmingdale, NY, USA). A total of 20 μg protein was run through 12% NuPAGE 4–12% Bis-Tris gel electrophoresis (Bio-Rad, Hercules, CA, USA) and transferred to a PVDF membrane (Bio-Rad). The blots were washed with 1x TBS (Bio-Rad) and with 0.05% Tween 20 (Sigma-Aldrich), blocked in 5% BSA (Santa Cruz) and incubated overnight at 4°C with primary antibodies for CD9, CD63, and CD81 (1:1000; Santa Cruz). Next, the blots were washed in TBST and incubated for 1 hour with goat anti-mouse horseradish peroxidase-conjugated secondary antibody (1:10000; Santa Cruz) followed by treatment with chemiluminescence reagent (BrightStar™ Femto HRP Chemiluminescent Substrate Kit). β-Actin is used as a control.

Erk Signaling Inhibition:

U0126, a highly selective inhibitor of MEK1/2 was purchased from Cell Signaling and dissolved in dimethylsulfoxide (DMSO) at a stock concentration of 10 mM, according to the manufacturer's protocol. To confirm the involvement of MEK signaling in exosome-mediated effects on hDPSCs, cells were pre-treated with the indicated concentration (10 uM) of U0126 or an equal volume of DMSO for 30 minutes. Subsequently, 5 μg/mL MDPC-EXO or an equal volume of PBS was added to the culture medium of hDPSCs, and cultured for 15 minutes. Western blotting was then performed as described above.

Nanoparticle Tracking Analysis (NTA):

The average hydrodynamic diameter and concentration of exosomes were characterized by NTA using a Nanosight NS3000 (Malvern) using the properties of light scattering and Brownian motion to obtain particle size distributions of samples in liquid suspension. Samples were agitated briefly in a sonic bath to break up aggregates, then exosomes were diluted in particle-free PBS and immediately analyzed. NTA was carried out using a 488 nm laser in scatter mode, using a syringe pump (Harvard Apparatus) to control flow. Five 60-second videos were recorded at a concentration sufficient to obtain a minimum of 200 tracks per video. Analysis was carried out using Malvern NanoSight NTA software v3.2.

Gene Expression Analysis:

Total RNA was isolated using Trizol Reagent (Thermo Fisher Scientific) according to the manufacturer's protocol [40]. The RNA was reverse transcribed using 5X All-In-One RT MasterMix (Applied Biological Materials Inc.) and subsequently amplified with PowerUp SYBR Green Master Mix (Thermo Fisher Scientific) using a 7500 Real-Time PCR System. Primers are shown in Table 1. Results were calculated by using the $2^{\Delta\Delta}$CT method [41]. GAPDH was used as an internal control to normalize the variability in expression levels.

Mineralization Assay (Alizarin Red Stain):

Calcium depositions in the extracellular matrix were observed using Alizarin Red staining after DPSCs were cultured for 14 days in odontogenic media, and for MDPCs after 1 week. The cells were then washed with PBS and fixed in 70% ethanol for 10 minutes at 4°C. DPSCs were stained with a solution of 1% alizarin red S (Sigma-Aldrich, St. Louis, MO, USA) for 5 mins at room temperature and washed with distilled water. The calcium content was also determined at day 14 using a colorimetric calcium assay kit (Calcium Reagent Set, Pointe Scientific, MI, USA), after disruption and incubation of samples overnight at 4°C with 1 N HCl.

Transwell Migration Assay:

Transwell migration assay was performed using a Transwell insert that contains a polycarbonate filter with 8 μm pore size (Corning Costar) DPSC cells were serum-starved for 24 h in DMEM prior to initiation of the experiment. 10×10^4 DPSCs suspended in 100uL serum-free DMEM were added to the 24-well upper chamber. The chambers were placed in 24-well plates, and either: 500 μL medium that contains carrier control (PBS), 1 μg/mL, 5 μg/mL or 10 μg/mL exosomes, was added to the bottom wells of the multi-well insert assembly. Cells were incubated at 37°C for 1 hour to allow cell migration through the membrane. Migrated cells were fixed in 95% ethanol and stained with crystal violet. The images were captured and analyzed with Image J software (NIH).

Immunofluorescence and Confocal Microscopy:

Cells cultured in monolayer were fixed in formaldehyde (4%) for 1 hour, then cell membranes were permeabilized with Triton-X (0.1%) for 5 minutes. After washing with PBS, the cytoskeleton was stained using Alexa-Fluor 555 phalloidin (F-actin, 1:35) in BSA (1%), per the manufacturer's guidelines. Mounting media containing DAPI was used to stain nuclei (ProLong Gold Anti-Fade). Constructs were observed using a laser confocal microscope (Nikon Eclipse C1).

Particle Sterilization:

For release tests, cell culture studies, and in vivo assessment, exosome-containing particles were sterilized by ethylene oxide.

Evaluation of Exosome Release from Particles:

The release profiles of exosome-loaded microspheres (EXO-MS) were evaluated in PBS (pH 7.4, 0.1 M). A known mass of particles was incubated in 1.0 mL PBS and shaken at 50 rpm at 37°C. At designated time points, the conditioned PBS was withdrawn and frozen at −80°C and replaced with fresh PBS. Nanoparticle Tracking Analysis was used to determine the concentration of exosomes in each aliquot, which can be plotted as a cumulative function of time to describe exosome release from polymer spheres.

Evaluation of Particle Degradation:

At prescribed time points, particles which had been incubated in PBS for release tests (described above) were removed and frozen, then lyophilized, to examine partic le

morphology as a function of degradation. Particles were gold coated and observed by SEM as described.

RNA Isolation from Released Exosomes:

Conditioned PBS from release profile experiments was centrifuged at 12,000 g for 90 minutes at 4°C to recover exosomes from release test aliquots. RNA contained within exosomes was extracted using a phenol-based extraction method similar to extracting RNA from cells [42]. Total RNA extraction was performed using TRIzol reagent (Invitrogen) according to the manufacturer's protocol. 750 μL TRIzol was added to each concentrated sample and mixed well to resuspend exosomes and incubated at room temperature. Protein was denatured by addition of chloroform, then RNA was precipitated using isopropanol, and dried with 70% ethanol, before being reconstituted in water. The concentration of RNA was assessed by absorbance at 260 nm using a Beckman DU640 Spectrophotometer.

In Vitro Efficacy of Controlled Release to Enhance Mineralization:

EXO-MS were incubated in media at a concentration of 0.25 mg/mL at 37°C. DPSCs were plated in triplicate (50,000 cells/well) into 24-well plates and cultured to confluence. Cells were treated with EXO-MS eluent for two weeks, changing the conditioned media every two days with media conditioned by the EXO-MS.

Subcutaneous Implantation in Mice:

EXO-MS were immobilized onto poly(L-lactic acid) (PLLA) nanofibrous (NF) scaffolds, which serve as a 3D matrix for cells. PLLA NF scaffolds were fabricated by a combination of thermally induced phase separation and sugar porogen leaching techniques, described by our group previously [43]. Briefly D-fructose was emulsified in hot mineral oil containing Span80, a surfactant, and cooled quickly to produce sugar spheres. Spheres were collected, washed with hexane to remove mineral oil, and sorted by size using molecular sieves. Spheres of size 250–425 μm, a size range shown to be advantageous for mineralized tissue formation [44], were assembled into a template and annealed at 37°C. Hexane was removed with a vacuum, and poly(L-lactic acid) (10% w/v in THF) was cast into the template and frozen at −80°C to induce thermally induced phase separation, resulting in nanofibers. After 48 hours, THF was exchanged with hexane, and sugar spheres were leached from the scaffold using water. Scaffolds were cut to 5 mm diameter and 2 mm thickness. 600 μg exosomes were incorporated into 1.0 mg polymer microspheres (PLGA(85/15)-PEG-PLGA(85/15), 5k). Approximately 1.25 mg exosome-containing microspheres were used for each scaffold to achieve approximately 1.0 mg microspheres immobilization on each scaffold (considering microsphere loss in the process) using a modified post-seeding method [45, 46]. Briefly, particles were suspended in hexane with 0.1% Span80, then dried in a vacuum. Once dry, particles were resuspended in a THF-hexane solution (3% v/v THF). 12 μL of EXO-MS solution was aliquoted dropwise onto scaffolds, and scaffolds were placed on a rocker for 30 minutes at a low speed. This was repeated multiple times on each side, allowing the solvent to evaporate and particles to attach between aliquots such that a total of 1.25 mg of particles were used for each scaffold, sufficient for 250,000 cells. Scaffolds were left to dry in a vacuum chamber until a constant mass was reached (4 days).

After the controlled release system was validated *in vitro*, constructs containing EXO-MS were seeded with 2.50×10^5 primary mouse DPSCs and implanted in subcutaneous pockets on the back of mice, four constructs per mouse, for six weeks (n=4 per group). 8- to 10-week-old male C57BL6 mice (Jackson Laboratory) were anesthetized by inhalation of isoflurane (3–5% induction, 0.5–2% maintenance). A 2-inch dorsal incision was made on the disinfected back, where four pockets were made using blunt dissection, two on each side of the incision. One construct was placed in each pocket, randomly for each group (n=4/group). Pain was managed by subcutaneous injection of carprofen (5 mg/kg) for 48 hours post-surgery.

Samples were harvested at 6 weeks for histologic and gene expression analyses. Samples were fixed in 4% paraformaldehyde (PFA) for three days and embedded in paraffin for histological sectioning (5 μm). This animal procedure was approved by the Institutional Animal Care & Use Committee (IACUC) at the University of Michigan.

Rat Pulpotomy Model:

Male Sprague Dawley rats (Charles River, 225–250 g, 8 weeks old) were subjected to a bilateral first maxillary molar pulpotomy to assess the ability of EXO-MS to cause tertiary dentin formation after insult [47]. Rats were anesthetized by inhalation of isoflurane gas (3–5% induction, 1–2% maintenance), and immobilized in a custom-built rat dental bed, inspired by previous literature in mice [48] which allowed for restraint, proper head positioning, and maintained isoflurane flow to the animal throughout the procedure. The mouth was held open by surgical retractor, and both maxillary first molars were disinfected with povidone-iodine. A 1/4C FG round diamond bur (Nobel Biocare) and dental handpiece was used to make a 0.5 mm class I defect in the occlusal surface of the tooth. Sterile saline (0.9%) was used for cooling and removal of debris. A size 15 endodontic K-File (Kerr) was used to expose the dental pulp. Hemostasis was controlled with a sterile cotton pellet.

To assess the ability of the controlled release of exosomes to induce tertiary dentin formation, rats were treated with either no particles, blank MS (polymer only, no exosomes), DPSC-EXO-loaded EXO-MS, or MDPC-EXO-loaded EXO-MS (n=4/group). 600 μg exosomes were incorporated into 1.0 mg polymer microspheres (PLGA(85/15)-PEG-PLGA(85/15), 5k). To cap one tooth, 1.0 mg polymer exosome-loaded microspheres were constituted in 100 μL ethanol, agitated on a shaker at room temperature for 30 minutes, then centrifuged and ethanol replaced, three times, to increase the hydrophilicity of the surface. On the final wash, particles were constituted in 50 μL PBS (5% PEG-2000, 0.1M PBS, pH 7.4, 1% Na_2HPO_3) and allowed to swell into a paste which was placed in the defect using a dental excavator and dried gently with air. Defects were closed with glass-ionomer cement (Fuji GC). Maxillary first molars capped with GI cement only were used as a negative control. Opposing cusp tips of mandibular first molars were removed with the 1/4C bur to relieve occlusion. Animals were given carprofen to manage pain (5 mg/kg) for 48 hours following surgery. This animal procedure was approved by the IACUC at the University of Michigan.

Animals were sacrificed at 6-weeks post-surgery; both maxillary first molars and surrounding alveolar bone was surgically dissected. Samples were fixed in 4% PFA for one

week then demineralized in 4% ethylenediaminetetraacetic acid (EDTA) for 8 weeks at room temperature, prior to paraffin embedding for histological sectioning.

Histological Analysis:

Samples were fixed in 4% PFA and demineralized (rat molars only). After dehydration, the samples were embedded in paraffin. Serial sections (5 μm) were cut and stained according to standard protocols for: hematoxylin and eosin (H&E) and Masson's trichrome staining. Stained sections were evaluated with a light microscope equipped with a camera (Olympus BX51).

Statistical Methods:

All data are reported in the form: mean ± standard deviation. The Student's t-test was used to determine statistical significance of observed differences between experimental groups, where $p < 0.05$ is used to determine significance. Statistical analysis was carried out in GraphPad Prism v8 and IBM SPSS v23.0.

Results

Isolation of Exosomes from Dental Pulp Stem Cells (DPSCs) and Immortalized Murine Odontoblasts (MDPC-23):

Primary human dental pulp stem cells (hDPSCs) were isolated from adult human teeth and cultured under odontogenic conditions for two weeks; immortalized murine odontoblasts from the MDPC-23 cell line were likewise cultured under odontogenic conditions. The mineralization status of both cell types was confirmed by positive Alizarin Red staining. Following positive Alizarin Red staining, conditioned media (CM) was collected every two days and their exosomes were isolated according to a standard protocol (hDPSC-derived exosomes = DPSC-EXO; MDPC-23-derived exosomes = MDPC-EXO) [38]. The exosome fractions were physically and molecularly analyzed to determine the content and purity of the isolate according to standard methods [49]. Nanoparticle tracking analysis (NTA) results show that the samples are relatively monodisperse with an average hydrodynamic diameter of 135 nm (Sup Fig 1A, B). Exosome-specific surface markers are significantly enriched in the isolated exosome fraction compared to the total cell lysate, whereas β-actin is enriched in the cell lysate but not significantly enriched in the exosome fraction (Sup Fig 1C, D). Freshly isolated DPSC-EXO and MDPC-EXO were fluorescently labelled with a lipophilic fluorophore (DiO, green) and incubated with hDPSCs for 30 minutes, separately. Visualization by confocal microscopy shows that exosomes are rapidly up-taken into the cytoplasm of cells based on colocalization with cell bodies (Sup Fig 1E, F).

Characterizing the Therapeutic Properties of Dentinogenic Exosomes

DPSC-EXO were previously demonstrated to induce odontogenic differentiation of DPSCs in vitro [25, 26]; we confirmed that exosomes derived from primary human DPSCs cultured in odontogenic media indeed induced the differentiation of DPSCs towards an odontogenic phenotype (Fig 1A, B). After 7 days, treatment by DPSC-EXO (5 μg/mL) induced significant upregulation of characteristic dentinogenic genes: BSP, DSPP, VEGF—compared to culture in odontogenic media alone (Fig 1A). DPSC-EXO treatment also significantly

increased mineralization after 14 days, compared to odontogenic and growth media controls, determined by colorimetric assay (Fig 1B). Doses greater than 5 μg/mL showed little difference from a 5 μg/mL dose, indicating saturation. MDPC-derived exosomes have not previously been studied; we demonstrate that they too upregulate characteristic odontogenic gene expression of DPSCs (Fig 1C). DPSC-EXO and MDPC-EXO both induce significant increases in mineralization (5 μg/mL) over odontogenic media alone after two weeks, with MDPC-EXO inducing the most mineralization as demonstrated by colorimetric assay (Fig 1D) and Alizarin Red staining (Fig 1E).

It is known that DPSC-EXO induce mineralization by upregulation of MAPK signaling [25]. Western blot analysis demonstrated that MDPC-EXO also upregulate Erk1/2 phosphorylation (5 μg/mL) in as little as 5 minutes *in vitro* (Fig 1F). Furthermore, MDPC-EXO upregulated phosphorylation of Erk1/2 and downstream RUNX2 protein expression, in a dose-dependent manner as assessed at 15 minutes (Fig 1G). U0126 was used to inhibit MAPK signaling in order to confirm its involvement in MDPC-EXO-mediated odontogenic differentiation. U0126 decreased levels of p-Erk1/2 and RUNX2 in hDPSCs; MDPC-EXO rescued this decrease to some extent, confirming MAPK signaling involvement (Fig 1H, I, J). Additionally, the normalized data of the MDPC-EXO groups (without U0126 treatment) in Fig 1I & J quantitatively confirm that MDPC-EXO enhance p-Erk1/2 and RUNX2 protein levels compared to respective DMSO control groups.

Feasibility of Sustained Exosome Delivery to Catalyze Tissue Neogenesis

We hypothesized that exosomes eluted from a synthetic delivery vehicle would induce migration of endogenous cells to repair breached dentin. To probe the migratory potential of dentinogenic exosomes, hDPSCs were seeded on the top of a trans-well insert, above odontogenic media supplemented with various doses of DPSC-EXO (0–10 ug/mL). hDPSCs migrated towards the DPSC-EXO-containing media in a dose dependent manner, in as little as one hour *in vitro* (Fig 2A, B), demonstrating the migratory potential of DPSC-EXO.

Typical *in vitro* experiments are performed where fresh exosomes are supplemented in the culture media constantly throughout the duration of the experiment. We were interested in the effect of a single dose versus sustained exposure to DPSC-EXO on the pro-odontogenic mineralization capacity of hDPSCs, which could be achieved *in vivo* through a sustained release delivery platform. hDPSCs were exposed to DPSC-EXO for a prescribed time period, then switched to odontogenic media alone, as shown schematically in Fig 2C; odontogenic and growth media are positive and negative controls, respectively. Even a single dose of DPSC-EXO (72 hours culture then odontogenic media alone) resulted in a greater degree of mineralization compared to cells cultured in odontogenic media alone. The sustained exposure to DPSC-EXO increased mineralization by almost two-times (Grp 4), compared to odontogenic media alone, in a time-dependent manner (Fig 2D).

Polymeric Encapsulation of DPSC-EXO by a Self-Assembling Triblock Copolymer

We designed a novel platform for the encapsulation of dentinogenic exosomes into biodegradable polymeric microspheres, using a modified double emulsion method [30]. The double emulsion consists of three phases: an inner water phase which contains exosome

cargo (DPSC-EXO), a middle organic solvent phase containing a biodegradable polymer dissolved in dichloromethane (DCM), and an outer continuous phase of polyvinyl alcohol (PVA) surfactant dissolved in water (1% w/v), shown schematically in Fig 2E. Poly(lactic-*co*-glycolic acid)-*block*-poly(ethylene glycol)-*block*-poly(lactic-*co*-glycolic acid) (PLGA-PEG-PLGA), an amphiphilic triblock copolymer (Fig 2F), was synthesized and its composition was confirmed by nuclear magnetic resonance spectroscopy and molecular weight by gel permeation chromatography (Sup Fig 2). Mechanical emulsion facilitated the formation of exosome-loaded microspheres (EXO-MS) *in situ* – first, the exosome solution was emulsified in PLGA-PEG-PLGA/DCM solution (5% w/v) for a prescribed time period. Then this water-oil (w/o) emulsion was emulsified in 1% w/v PVA. DCM was evaporated to yield solid polymeric spheres. Laser diffraction (Mastersizer 2000) measurements of EXO-MS size show a broad distribution of particles ranging from 25–75 μm in diameter ($d_{av\ g}$ = 42 μm, Fig 2G). Scanning electron microscopy (SEM) visualization of EXO-MS shows consistent spherical microparticles with a smooth surface texture (Fig 2H). The internal morphology of EXO-MS shows a "sphere-in-sphere" morphology (Fig 2H) when the PEG:PLGA ratio is 1:4. At a PEG:PLGA ratio of 1:10, resulting particles form uniform, large spheres with smooth surfaces, however no internal pockets characteristic of the "sphere-in-sphere" morphology result. At a ratio of 2:3, resulting polymer disks are flat, non-uniformly shaped and their size is broadly distributed, lacking an internal architecture (Sup Fig 3). The duration of the first w/o emulsion is important in achieving a smooth surface texture; particle dispersity changes with emulsion time (Sup Fig 4A). PVA surfactant results in smoother particle morphology, likely due to its nonionic nature (Sup Fig 4B). As anticipated, increasing the concentration of PVA decreases particle dispersity (Sup Fig 4C). However, PVA is known to be cytotoxic at high concentrations.

To probe at the mechanism by which PLGA-PEG-PLGA results in a "sphere-in-sphere" EXO-MS morphology, we synthesized copolymer blocks with fluorescent end-group probes (Sup Fig 5). EXO-MS were fabricated from PLGA-PEG-PLGA mixed with those fluorescent polymers and fluorescently labelled exosomes and visualized by confocal microscopy (Fig 3A). EXO-MS consist largely of PLGA (red). PEG segments (blue) form spherical or more complex pockets within the PLGA MS. DPSC-EXO (green) tend to co-localize with PEG in these inner-sphere pockets. The PEG is the hydrophilic segment of the PLGA-PEG-PLGA copolymer, which was designed to interface with the aqueous droplets containing exosomes inside the hydrophobic PLGA body of a microsphere driven by hydrophilic/hydrophobic self-assembly. Therefore, we anticipated exosomes to overlap significantly with the PEG domains. Diblock monomethyl ether-poly(ethylene-glycol)-*block*-poly(lactic-*stat*-*co*-glycolic acid) (H_3C-PEG-PLGA) was synthesized to the same molecular weight and PEG-segment molecular weight as PLGA-PEG-PLGA. Triblock PLGA-PEG-PLGA formed uniform spheres with smooth surfaces, however H_3C-PEG-b-PLGA formed deflated spherical particles which lacked uniformity or a smooth surface texture (Fig 3B).

Sustained Release Kinetics of DPSC-EXO from EXO-MS in vitro

EXO-MS were fabricated from six different chemical formulations of triblock PLGA-PEG-PLGA. The hydrophilicity of the PLGA block is modulated by the lactide/glycolide

composition, synthesized at: 100/0, 85/15, 70/30, and 50/50. Additionally, the molecular weight is varied between 5 kDa and 30 kDa. EXO-MS are incubated in phosphate buffered saline (PBS) at 37°C. Aliquots are removed at prescribed timepoints to analyze dentinogenic exosome concentration in the particle eluent and replaced with fresh PBS. Cumulative release from EXO-MS shows an initial burst within the first 72 hours, then the release becomes more linear (Fig 4A–C). Not surprisingly, higher molecular weights and higher lactide/glycolide ratios resulted in slower release rates and reduced burst release amounts. $PL_{85}G_{15}A$-PEG-$PL_{85}G_{15}A$ (5 kDa) was chosen for subsequent studies because of its relatively longer sustained release up to 10 weeks *in vitro*. Initially, 27% of loaded exosomes were released in the initial 72 hours, then DPSC-EXO were released at a rate of 0.8% per day. Exosome eluent is analyzed by NTA to determine release as a function of particle number; the exosomes maintain their characteristic hydrodynamic diameter and monodispersity centered around $d_{av\ g}$ = 115 nm throughout release (Fig 4D, Sup Fig 6). EXO-MS were fabricated with fluorescently labelled exosomes; EXO-MS were incubated for two weeks in PBS, changing the PBS every two days. At day 14, PBS was changed for odontogenic media and EXO-MS were left to condition the media. hDPSCs were incubated with EXO-MS-conditioned odontogenic media for 30 minutes; the uptake of fluorescent dentinogenic exosomes, released from EXO-MS, was visualized by confocal microscopy (Fig 4E).

Scanning electron micrographs of EXO-MS are taken at various time points throughout degradation (Sup Fig 7). Initially, EXO-MS maintain their intact structure up to two weeks, as the outer shell is degraded and becomes increasingly porous. By one month, the microspheres have deformed from their original shape into an irregular shape with a rough texture and less-defined internal “sphere-in-sphere” morphology.

Prior to use *in vitro* and *in vivo*, EXO-MS were sterilized by ethylene oxide gas, then with 70% ethanol. Neither ethanol nor methanol caused significant release of DPSC-EXO, even up to 4 weeks (Sup Fig 8A). After two weeks incubation in ethanol (changed every other day), ethanol was exchanged for water, and EXO-MS immediately began releasing DPSC-EXO as anticipated (Sup Fig 8B).

In Vitro Integrity and Bioactivity of Exosomes Eluted from Polymer Microspheres

Exosomes are biologically derived liposomes, and known to aggregate *in vitro*, particularly in highly concentrated suspensions and during freezing. We investigated the stabilization of encapsulated exosomes by D-trehalose in EXO-MS fabrication, previously shown to stabilize exosome lyophilization [50]. Scanning electron micrographs of fixed EXO-MS eluent show that D-trehalose incorporated in the fabrication of EXO-MS (2 mM) helps to minimize the size of exosome aggregates, compared to those encapsulated without any stabilization, judged by morphology (Fig 5). Trehalose-stabilized exosomes maintain their characteristic spherical shape, size, and membrane integrity. The lipid membrane plays an important role in protecting the nucleic acid cargo of exosomes, largely made up of miRNA, responsible for their physiologic effects *in vitro* and *in vivo*. At each time point in *in vitro* release assays, RNA cargo was extracted from therapeutic dentinogenic exosomes. The amount of RNA extracted from exosome eluent matches well to exosome particle number,

from NTA, for all polymer compositions and molecular weights investigated (Fig 6, Sup Fig 9). While both diblock and triblock copolymers could efficiently encapsulate exosomes, diblock copolymers released cargo much quicker than triblock copolymers (Sup Fig 10).

hDPSCs were treated with eluent from either blank (unloaded) EXO-MS or EXO-MS loaded with DPSC-EXO, compared to odontogenic and growth media controls for 14 days *in vitro* to determine the bioactivity of dentinogenic exosomes after release and demonstrate feasibility. The controlled release of dentinogenic exosomes from EXO-MS significantly increased hDPSC calcium mineralization compared to blank EXO-MS and positive (odontogenic media) and negative (growth media) controls, determined by alizarin red staining (Fig 7A) and colorimetric calcium assay (Fig 7B). Increases in calcium mineralization were accompanied by upregulation in dentin sialophosphoprotein (DSPP), dentin matrix phosphoprotein 1 (DMP1) and bone sialoprotein (BSP) gene expression, characteristic of dentinogenesis and odontogenic differentiation (Fig 7C).

Subcutaneous Implantation of EXO-MS Induces DPSC Differentiation In Vivo

Blank EXO-MS, DPSC-EXO-loaded EXO-MS or MDPC-EXO-loaded EXO-MS (called DPSC-EXO-MS and MDPC-EXO-MS, respectively) were attached to nanofibrous tissue engineering scaffolds, separately, which serve as a three-dimensional matrix, as previously described [45]. Constructs were seeded with freshly isolated naïve mouse DPSCs (mDPSCs) and implanted subcutaneously in mice for six weeks. Harvested constructs were stained with hematoxylin and eosin; MDPC-EXO-MS and DPSC-EXO-MS constructs showed increased cellularity compared to Blank EXO-MS (Blank) (Fig 8A, B, C). Additionally, Masson's Trichrome staining demonstrated increased extracellular matrix production in DPSC-EXO-MS or MDPC-EXO-MS loaded cell-scaffold constructs, compared to Blank controls (Fig 8D, E, F). The sustained release of exosomes induced significant odontogenic differentiation in mDPSCs via both cargo types (MDPC-EXO and DPSC-EXO); upregulation of Runx2, osteocalcin (OCN), dentin sialophosphoprotein (DSPP) and collagen 1 (Col1a1) when compared to blank constructs (Fig 8G). No inflammation and minimal fibrous capsule formation were noted in histologic examinations.

Dentin Defect Repair by EXO-MS in a Rat Pulp-Capping Model

EXO-MS were further assessed for their ability to stimulate tertiary dentin formation in a biomimetic way through the controlled release of pro-dentinogenic exosomes without transplantation of exogenous cells at the dentin-pulp interface. A 0.10 mm Class II defect was made on the occlusal surface of bilateral maxillary molars of healthy 8- to 10-week-old male rats (Sprague Dawley, Charles River). DPSC-EXO-MS with glass ionomer resin, MDPC-EXO-MS with glass ionomer resin, blank EXO-MS with glass ionomer resin, or glass ionomer resin alone (clinical standard, as a control) were used to treat defects. Six weeks after treatment, maxillary molars were dissected *en bloc* and buccal-labial serial sections were cut for histological analyses. Some reparative tertiary dentin formation was noted in all treatment groups, to varying degrees. The sustained local release of DPSC-EXO and MDPC-EXO at the pulp interface resulted in more complete dentin healing and strong dentin bridge formation after six weeks *in vivo* (n=4 per group) (Fig 9). GI-only and blank EXO-MS-treated teeth show incomplete dentin bridge formation with irregular dentin

morphology and minimal hard tissue formation. Exosome treated teeth, on the other hand, show characteristic dentinal-tubules and highly mineralized tissue with a rich collagen extracellular matrix as shown by Masson's trichrome staining, indicating deposition of highly collagenous neodentin (arrows, Fig 9). Streaks in the dentin near the edges of the defect are characteristic of tertiary dentin which is differentiated from native secondary dentin (existing) tooth structure. Some nondegraded polymer particles are found in the remaining capping material, partially lost during histological preparation. The PLGA-PEG-PLGA polymer itself does not have therapeutic benefit, demonstrated by blank EXO-MS controls. Careful examination of the histological slides did not show any sign of bacterial infection. The accelerated tertiary dentin bridge formation by controlled exosome release should be beneficial in preventing potential bacterial invasion in the long term.

Discussion

Novel methods which accelerate dentinogenesis in safe and efficacious ways to maintain the vitality of the dental pulp are critically important to advancing the field of restorative dentistry, ultimately allowing patients to preserve their natural dentition [6]. Interest in advanced biologic therapeutics such as exosomes requires innovative engineering strategies to deliver these complex drugs [51]. The objective of the present work is to develop a novel platform for the controlled release of dentinogenic exosomes directly at the pulp surface to catalyze tertiary dentin formation and accelerate dentin bridge formation in the restoration of carious lesions, and secondarily identify candidate exosomes to enhance reparative dentinogenesis. We have demonstrated for the first time that stem cell-derived exosomes can be efficiently encapsulated and released from biodegradable polymeric microspheres, allowing for their efficient therapeutic delivery, while maintaining their bioactivity. PLGA-PEG-PLGA microspheres with a smooth surface and diameters ranging from 30 to 70 μm were developed to efficiently encapsulate cell-derived exosomes through self-assembly. Dentinogenic exosomes were released over the course of 8–12 weeks. Additionally, we showed cross-species efficacy of exosomes derived from both primary human cells and immortalized animal cell lines in considerably accelerating the formation of healthy tertiary dentin in a rat direct pulp capping model by 6 weeks. We believe this is a promising platform technology for the controlled release of stem cell-derived exosomes, adaptable to many therapeutic applications.

DPSC-EXO are demonstrated to be pro-dentinogenic *in vitro* towards hDPSCs by exogenous administration [52]. We additionally determined that DPSC-EXO can facilitate the migration of hDPSCs in a dose-dependent manner, and that DPSC-EXO induce mineralization in an exposure-dependent manner. These findings led us to develop a controlled release platform that can be implanted at a defect site without the transplantation of exogenous stem cells, to facilitate the migration of endogenous DPSCs from the inner pulp chamber *and* guide their differentiation fate towards a specific regenerative outcome.

Exosomes, by their biologic nature, are more delicate than small molecules and this consideration mus t be built into fabrication protocols for their encapsulation [53]. We designed an amphiphilic triblock copolymer, PLGA-PEG-PLGA, with a distinct small hydrophilic segment flanked by two longer hydrophobic segments. We hypothesized that its

hydrophobic/hydrophilic self-assembly likely facilitates the compartmentalization of exosome-containing water droplets within the organic-phase polymer solution, leading to the "sphere-in-sphere" morphology seen in SEM and confocal microscopy images of EXO-MS. In this way the amphiphilic triblock copolymer participates in the self-assembly, with the PEG block to interface between the aqueous droplets containing exosomes and the hydrophobic PLGA shells of the inner spheres. There are often multiple inner microspheres in the larger PLGA-PEG-PLGA microspheres (often from tens to greater than a hundred of microns). Each of the inner spheres likely contains multiple exosomes based on the size of the inner spheres (a few to tens of microns) and the size of the exosomes (50–150 nm). There also may be multilayered PLGA-PEG-PLGA microspheres, with exosomes in the hydrophilic cores or hydrophilic intermediate shells. In reality, the exosome-containing aqueous domains can take either a more defined regular morphology or more complex morphologies depending on the polymer composition, molecular weight, the viscosities of the two phases, and the fabrication parameters etc. The PEG block presumably can also present itself at the outer surface of inner spheres and the outer surface of the entire solid spheres to stabilize the system during fabrication. We attribute the sustained release properties of EXO-MS to this internal architecture which creates miniature reservoirs throughout the construct. As PLGA is hydrolyzed and EXO-MS become hydrated, PEG retains water within the PLGA MS to enable degradation from inside out along with degradation from outside in to release their exosome cargo. As the pore openings reach sufficient size, exosomes are able to diffuse out. Since PLLA is more hydrophobic and more densely packed than PLGA copolymers, water penetrates slower and PLLA spheres degrade slower, which reduces both the burst release and the rate of sustained exosome release.

As demonstrated in this study, the odontogenic exosomes have multiple functions including inducing stem cell migration, promoting odontogenic differentiation, enhancing mineralization, and facilitating tertiary dentin bridge formation. It often takes many weeks to form such mineralized tissue. Ten weeks is a reasonable duration for larger animal models or potential future clinical application. Importantly, the selected PLGA (85/15, 5kD) allows both the longer term and relatively higher exosome release rate during the sustained release period, which is anticipated to present high biological activities.

Herein we also demonstrated that exosomes derived from an immortalized animal cell line (MDPC-23 odontoblasts) are capable of inducing mineralized tissue formation by human cells, and *in vivo* in a rat model. Cell line-derived exosomes may be advantageous in the future development of exosome-based therapies because of their cell maturity, consistency, and ability to be maintained in a stable phenotype. It is well established that exosome cargo is reflective of the donor cell identity and status [26]. Specifically, Wei demonstrated that exosomes derived from mid- and late-stage differentiated osteoblasts remarkably promoted osteoblast differentiation of bone marrow-derived stromal cells compared to exosomes derived from early-stage osteoblasts [54]. The late stage and consistency of MDPC-23 odontoblasts may be favorable towards efficient scaling of exosome-based therapies, compared to guided differentiation of primary cells preprequisite to exosome isolation

A key challenge in engineering drug delivery strategies is to stabilize the therapeutic agent to maintain its bioactivity [55]. Here we explored the potential of D-trehalose, a hydrophilic

disaccharide, to act as a spacer between DPSC-EXO during their confinement and polymeric encapsulation [50]. We hypothesized that sufficient concentration of Trehalose may limit aggregation, lending to a more uniform release of exosomes from EXO-MS. Trehalose is a cost-effective additive for preventing aggregation of exosomes in our novel delivery platform. It is a non-reducing disaccharide sugar which is used as a cryoprotectant industrially. D-Trehalose was previously used as an exosome cryopreservative at a concentration of 25 mM, cited to stabilize proteins, cell membranes, and liposomes by decreasing intracellular ice formation and prevent protein aggregation [50]. Here we demonstrate that D-Trehalose added to the discrete aqueous phase at a concentration as low as 2 mM has stabilizing effects to minimize exosome aggregation during both the encapsulation and release process. At such a low concentration D-trehalose does not likely have significant negative metabolic or therapeutic consequences.

After fabrication and lyophilization, EXO-MS are easily stored and sterilized before use. After mixing with Na_2HPO_4 and PEG to make a paste, the EXO-MS paste was easily placed at the pulp surface and covered with glass ionomer (GI) cement with a dental excavator. Our novel treatment modality is both efficacious and easy to handle, similar in texture to existing dental materials. Throughout the *in vivo* experiment, all rats remained in good health with no significant changes in weight or overall well-being. Molar teeth remained intact without signs of fracture or occlusal stress, allowing them to be retrieved complete with surrounding maxillary bone. EXO-MS treated teeth show formation of a tubular tertiary dentin bridge after only six weeks *in vivo*. Tubularity is a distinguishing feature between reactionary and reparative dentin; reactionary dentin has similar integrity to primary and secondary native dentins, while reparative dentin is less organized and creates less of a barrier to the pulp [56]. Additionally, EXO-MS does not cause dystrophic calcification in the pulp where GI-treatment has the potential to result in small microparticles of calcium and mineral from the cement to be incorporated into the pulp or cause inflammation. EXO-MS treated teeth did not show signs of inflammation, abscess, or necrosis, likely due to the accelerated healing of the dentin bridge which prevented significant bacterial invasion. Sustained inflammation damages the pulp tissue and prevents further repair by downregulating recruitment and differentiation of naïve DPSCs from the inner pulp [57].

A variety of pulp capping materials have been developed to date with varied use cases and clinical prognoses [6]. Calcium hydroxide ($Ca(OH)_2$) paste is the most commonly used pulp capping material in clinic [58]. While it is cost-effective, it leads to tunnel defects in the dentin bridge which increase its permeability and is known to cause severe pulp chamber inflammation for up to three months, which slows the healing process and does not seal well particularly in cases with pulpal bleeding. Additionally, it is not recommended for use in pediatric patients because of inflammatory concerns [58]. Mineral trioxide aggregate (MTA), made of natural Portland cement, is another commercially available product which leads to less pulp inflammation and better long-term pulp vitality than $Ca(OH)_2$; however, it is difficult to handle with a long setting time, expensive, and causes coronal tooth discoloration. More recent advances including bioaggregate and biodentine are both expensive and have poor handling properties. However, their synthetic nature does not cause mineral leaching and tooth discoloration. Calcium and mineral-based cements degrade very slowly in the oral cavity, which slows the process of tissue ingrowth and replacing the

material with native dentin. Dentin forms around these mineral spherulites and tends to be irregular, as seen in GI-only and blank EXO-MS treated rats. Glass ionomer (GI) and zinc oxide eugenol (ZOE) resins are used to cover defects and to seal them off from the external environment, are easy to handle, and can be used in pediatric, adult, and geriatric patients without concern. However, reparative dentin forms slowly over time, the material does not catalyze its formation efficiently leaving a potential for bacterial infiltration and infection. PLGA-PEG-PLGA EXO-MS which stimulate dentin repair in a biomimetic way, paired with a sealing agent like GI, are ideal because they are easy to handle, cost-effective, and cause neither inflammation nor discoloration. We did not see any bacterial infection. The exosome-accelerated tertiary dentin bridge formation should be beneficial in preventing bacterial invasion in the long term.

Exosomes recapitulate the beneficial paracrine properties of stem cells, without concerns of immunogenicity [59]. Additionally, there are manufacturing, and regulatory advantages associated with exosome-based therapies, compared to treatment with stem cells particularly when considering cell line-derived exosomes [60]. In this way, controlled release of exosomes from EXO-MS is able to stimulate the migration of endogenous DPSCs and guide their differentiation towards secretory odontoblasts, inducing tertiary dentin bridge formation in a biomimetic way.

Conclusions

In conclusion, we have demonstrated that an amphiphilic triblock copolymer is capable of efficiently encapsulating and subsequently releasing cell-derived exosomes in a sustained fashion, at a local dental pulp defect site, to enhance tissue neogenesis catalyzed by the nucleotide cargo of exosomes. Specifically, utilizing our novel EXO-MS delivery platform, exosomes derived from human dental pulp stem cells (hDPSCs) and immortalized murine odontoblasts (MDPC-23 cell line) were released at the exposed pulp interface *in vivo* and induced migration of resident DPSCs and their differentiation into odontoblasts to secrete a reactionary tertiary dentin bridge and prevent tooth necrosis. Cell-type specific exosomes cultured under specific conditions are an important tool for eliciting specific responses from endogenous stem cells. EXO-MS has the potential to be a useful delivery vehicle for cell-derived exosomes across a number of therapeutic applications.

Supplementary Material

Refer to Web version on PubMed Central for supplementary material.

Acknowledgements

The authors are grateful to University of Michigan Dental Stores, Stephanie Christau (Biointerfaces Institute Nanotechnicum, UM), Chris Strayhorn (University of Michigan School of Dentistry Histology Core), Taocong Jin (University of Michigan School of Dentistry Molecular Biology Core), Owen Neil (Electron Microbeam Analysis Laboratory), Prof. Helena Ritchie (University of Michigan School of Dentistry, Department of Cariology) for equipment assistance and fruitful discussion.

Funding

This work was supported by the National Institute of Dental and Craniofacial Research (National Institutes of Health) R01-DE02232 (PXM) and R01-DE27662 (PXM) research grants, and T32-DE007075 training grant fellowship (WBS); University of Michigan Rackham Graduate School graduate student research grant (WBS). Zhen Zhang was partially supported for living expenses by China Scholarship Council CSC201706240064 (ZZ, stipend).

References

[1]. Vos T, Abajobir AA, Abate KH, Abbafati C, Abbas KM, Abd-Allah F, Abdulkader RS, Abdulle AM, Abebo TA, Abera SF, Aboyans V, Abu-Raddad LJ, Ackerman IN, Adamu AA, Adetokunboh O, Afarideh M, Afshin A, Agarwal SK, Aggarwal R, Agrawal A, Agrawal S, Ahmadieh H, Ahmed MB, Aichour MTE, Aichour AN, Aichour I, Aiyar S, Akinyemi RO, Akseer N, Al Lami FH, Alahdab F, Al-Aly Z, Alam K, Alam N, Alam T, Alasfoor D, Alene KA, Ali R, Alizadeh-Navaei R, Alkerwi A.a., Alla F, Allebeck P, Allen C, Al-Maskari F, Al-Raddadi R, Alsharif U, Alsowaidi S, Altirkawi KA, Amare AT, Amini E, Ammar W, Amoako YA, Andersen HH, Antonio CAT, Anwari P, Ärnlöv J, Artaman A, Aryal KK, Asayesh H, Asgedom SW, Assadi R, Atey TM, Atnafu NT, Atre SR, Avila-Burgos L, Avokphako EFGA, Awasthi A, Bacha U, Badawi A, Balakrishnan K, Banerjee A, Bannick MS, Barac A, Barber RM, Barker-Collo SL, Bärnighausen T, Barquera S, Barregard L, Barrero LH, Basu S, Battista B, Battle KE, Baune BT, Bazargan-Hejazi S, Beardsley J, Bedi N, Beghi E, Béjot Y, Bekele BB, Bell ML, Bennett DA, Bensenor IM, Benson J, Berhane A, Berhe DF, Bernabé E, Betsu BD, Beuran M, Beyene AS, Bhala N, Bhansali A, Bhatt S, Bhutta ZA, Biadgilign S, Bicer BK, Bienhoff K, Bikbov B, Birungi C, Biryukov S, Bisanzio D, Bizuayehu HM, Boneya DJ, Boufous S, Bourne RRA, Brazinova A, Brugha TS, Buchbinder R, Bulto LNB, Bumgarner BR, Butt ZA, Cahuana-Hurtado L, Cameron E, Car M, Carabin H, Carapetis JR, Cárdenas R, Carpenter DO, Carrero JJ, Carter A, Carvalho F, Casey DC, Caso V, Castañeda-Orjuela CA, Castle CD, Catalá-López F, Chang H-Y, Chang J-C, Charlson FJ, Chen H, Chibalabala M, Chibueze CE, Chisumpa VH, Chitheer AA, Christopher DJ, Ciobanu LG, Cirillo M, Colombara D, Cooper C, Cortesi PA, Criqui MH, Crump JA, Dadi AF, Dalal K, Dandona L, Dandona R, das Neves J, Davitoiu DV, de Courten B, De Leo DD, Defo BK, Degenhardt L, Deiparine S, Dellavalle RP, Deribe K, Des Jarlais DC, Dey S, Dharmaratne SD, Dhillon PK, Dicker D, Ding EL, Djalalinia S, Do HP, Dorsey ER, dos Santos KPB, Douwes-Schultz D, Doyle KE, Driscoll TR, Dubey M, Duncan BB, El-Khatib ZZ, Ellerstrand J, Enayati A, Endries AY, Ermakov SP, Erskine HE, Eshrati B, Eskandarieh S, Esteghamati A, Estep K, Fanuel FBB, Farinha CSES, Faro A, Farzadfar F, Fazeli MS, Feigin VL, Fereshtehnejad S-M, Fernandes JC, Ferrari AJ, Feyissa TR, Filip I, Fischer F, Fitzmaurice C, Flaxman AD, Flor LS, Foigt N, Foreman KJ, Franklin RC, Fullman N, Fürst T, Furtado JM, Futran ND, Gakidou E, Ganji M, Garcia-Basteiro AL, Gebre T, Gebrehiwot TT, Geleto A, Gemechu BL, Gesesew HA, Gething PW, Ghajar A, Gibney KB, Gill PS, Gillum RF, Ginawi IAM, Giref AZ, Gishu MD, Giussani G, Godwin WW, Gold AL, Goldberg EM, Gona PN, Goodridge A, Gopalani SV, Goto A, Goulart AC, Griswold M, Gugnani HC, Gupta R, Gupta R, Gupta T, Gupta V, Hafezi-Nejad N, Hailu GB, Hailu AD, Hamadeh RR, Hamidi S, Handal AJ, Hankey GJ, Hanson SW, Hao Y, Harb HL, Hareri HA, Haro JM, Harvey J, Hassanvand MS, Havmoeller R, Hawley C, Hay SI, Hay RJ, Henry NJ, Heredia-Pi IB, Hernandez JM, Heydarpour P, Hoek HW, Hoffman HJ, Horita N, Hosgood HD, Hostiuc S, Hotez PJ, Hoy DG, Htet AS, Hu G, Huang H, Huynh C, Iburg KM, Igumbor EU, Ikeda C, Irvine CMS, Jacobsen KH, Jahanmehr N, Jakovljevic MB, Jassal SK, Javanbakht M, Jayaraman SP, Jeemon P, Jensen PN, Jha V, Jiang G, John D, Johnson SC, Johnson CO, Jonas JB, Jürisson M, Kabir Z, Kadel R, Kahsay A, Kamal R, Kan H, Karam NE, A. Karch, Karema CK, Kasaeian A, Kassa GM, Kassaw NA, Kassebaum NJ, Kastor A, Katikireddi SV, Kaul A, Kawakami N, Keiyoro PN, Kengne AP, Keren A, Khader YS, Khalil IA, Khan EA, Khang Y-H, Khosravi A, Khubchandani J, Kiadaliri AA, Kieling C, Kim YJ, Kim D, Kim P, Kimokoti RW, Kinfu Y, Kisa A, Kissimova-Skarbek KA, Kivimaki M, Knudsen AK, Kokubo Y, Kolte D, Kopec JA, Kosen S, Koul PA, Koyanagi A, Kravchenko M, Krishnaswami S, Krohn KJ, Kumar GA, Kumar P, Kumar S, Kyu HH, Lal DK, Lalloo R, Lambert N, Lan Q, Larsson A, Lavados PM, Leasher JL, Lee PH, Lee J-T, Leigh J, Leshargie CT, Leung J, Leung R, Levi M, Li Y, Li Y, Li Kappe D, Liang X, Liben ML, Lim SS, Linn S, Liu PY, Liu A, Liu S, Liu Y, Lodha R, Logroscino G, London SJ, Looker KJ, Lopez AD, Lorkowski S, Lotufo PA, Low N, Lozano R, Lucas TCD, Macarayan ERK, Magdy Abd El Razek H, Magdy Abd El Razek M, Mahdavi M, Majdan M, Majdzadeh R, Majeed A, Malekzadeh R, Malhotra R, Malta DC, Mamun AA, Manguerra H, Manhertz T, Mantilla A, Mantovani LG, Mapoma CC,

Marczak LB, Martinez-Raga J, Martins-Melo FR, Martopullo I, März W, Mathur MR, Mazidi M, McAlinden C, McGaughey M, McGrath JJ, McKee M, McNellan C, Mehata S, Mehndiratta MM, Mekonnen TC, Memiah P, Memish ZA, Mendoza W, Mengistie MA, Mengistu DT, Mensah GA, Meretoja TJ, Meretoja A, Mezgebe HB, Micha R, Millear A, Miller TR, Mills EJ, Mirarefin M, Mirrakhimov EM, Misganaw A, Mishra SR, Mitchell PB, Mohammad KA, Mohammadi A, Mohammed KE, Mohammed S, Mohanty SK, Mokdad AH, Mollenkopf SK, Monasta L, Montico M, Moradi-Lakeh M, Moraga P, Mori R, Morozoff C, Morrison SD, Moses M, Mountjoy-Venning C, Mruts KB, Mueller UO, Muller K, Murdoch ME, Murthy GVS, Musa KI, Nachega JB, Nagel G, Naghavi M, Naheed A, Naidoo KS, Naldi L, Nangia V, Natarajan G, Negasa DE, Negoi RI, Negoi I, Newton CR, Ngunjiri JW, Nguyen TH, Nguyen QL, Nguyen CT, Nguyen G, Nguyen M, Nichols E, Ningrum DNA, Nolte S, Nong VM, Norrving B, Noubiap JJN, O'Donnell MJ, Ogbo FA, Oh I-H, Okoro A, Oladimeji O, Olagunju TO, Olagunju AT, Olsen HE, Olusanya BO, Olusanya JO, Ong K, Opio JN, Oren E, Ortiz A, Osgood-Zimmerman A, Osman M, Owolabi MO, Pa M, Pacella RE, Pana A, Panda BK, Papachristou C, Park E-K, Parry CD, Parsaeian M, Patten SB, Patton GC, Paulson K, Pearce N, Pereira DM, Perico N, Pesudovs K, Peterson CB, Petzold M, Phillips MR, Pigott DM, Pillay JD, Pinho C, Plass D, Pletcher MA, Popova S, Poulton RG, Pourmalek F, Prabhakaran D, Prasad NM, Prasad N, Purcell C, Qorbani M, Quansah R, Quintanilla BPA, Rabiee RHS, Radfar A, Rafay A, Rahimi K, Rahimi-Movaghar A, Rahimi-Movaghar V, Rahman MHU, Rahman M, Rai RK, Rajsic S, Ram U, Ranabhat CL, Rankin Z, Rao PC, Rao PV, Rawaf S, Ray SE, Reiner RC, Reinig N, Reitsma MB, Remuzzi G, Renzaho AMN, Resnikoff S, Rezaei S, Ribeiro AL, Ronfani L, Roshandel G, Roth GA, Roy A, Rubagotti E, Ruhago GM, Saadat S, Sadat N, Safdarian M, Safi S, Safiri S, Sagar R, Sahathevan R, Salama J, Saleem HOB, Salomon JA, Salvi SS, Samy AM, Sanabria JR, Santomauro D, Santos IS, Santos JV, Santric Milicevic MM, Sartorius B, Satpathy M, Sawhney M, Saxena S, Schmidt MI, Schneider IJC, Schöttker B, Schwebel DC, Schwendicke F, Seedat S, Sepanlou SG, Servan-Mori EE, Setegn T, Shackelford KA, Shaheen A, Shaikh MA, Shamsipour M, Shariful Islam SM, Sharma J, Sharma R, She J, Shi P, Shields C, Shifa GT, Shigematsu M, Shinohara Y, Shiri R, Shirkoohi R, Shirude S, Shishani K, Shrime MG, Sibai AM, Sigfusdottir ID, Silva DAS, Silva JP, Silveira DGA, Singh JA, Singh NP, Sinha DN, Skiadaresi E, Skirbekk V, Slepak EL, Sligar A, Smith DL, Smith M, Sobaih BHA, Sobngwi E, Sorensen RJD, Sousa TCM, Sposato LA, Sreeramareddy CT, Srinivasan V, Stanaway JD, Stathopoulou V, Steel N, Stein MB, Stein DJ, Steiner TJ, Steiner C, Steinke S, Stokes MA, Stovner LJ, Strub B, Subart M, Sufiyan MB, Sunguya BF, Sur PJ, Swaminathan S, Sykes BL, Sylte DO, Tabarés-Seisdedos R, Taffere GR, Takala JS, Tandon N, Tavakkoli M, Taveira N, Taylor HR, Tehrani-Banihashemi A, Tekelab T, Terkawi AS, Tesfaye DJ, Tesssema B, Thamsuwan O, Thomas KE, Thrift AG, Tiruye TY, Tobe-Gai R, Tollanes MC, Tonelli M, Topor-Madry R, Tortajada M, Touvier M, Tran BX, Tripathi S, Troeger C, Truelsen T, Tsoi D, Tuem KB, Tuzcu EM, Tyrovolas S, Ukwaja KN, Undurraga EA, Uneke CJ, Updike R, Uthman OA, Uzochukwu BSC, van Boven JFM, Varughese S, Vasankari T, Venkatesh S, Venketasubramanian N, Vidavalur R, Violante FS, Vladimirov SK, Vlassov VV, Vollset SE, Wadilo F, Wakayo T, Wang Y-P, Weaver M, Weichenthal S, Weiderpass E, Weintraub RG, Werdecker A, Westerman R, Whiteford HA, Wijeratne T, Wiysonge CS, Wolfe CDA, Woodbrook R, Woolf AD, Workicho A, Xavier D, Xu G, Yadgir S, Yaghoubi M, Yakob B, Yan LL, Yano Y, Ye P, Yimam HH, Yip P, Yonemoto N, Yoon S-J, Yotebieng M, Younis MZ, Zaidi Z, Zaki MES, Zegeye EA, Zenebe ZM, Zhang X, Zhou M, Zipkin B, Zodpey S, Zuhlke LJ, Murray CJL, Global, regional, and national incidence, prevalence, and years lived with disability for 328 diseases and injuries for 195 countries, 1990–2016: a systematic analysis for the Global Burden of Disease Study 2016, The Lancet, 390 (2017) 1211–1259.

[2]. Fisher J, Selikowitz H-S, Mathur M, Varenne B, Strengthening oral health for universal health coverage, The Lancet, 392 (2018) 899–901.

[3]. Hilton TJ, Keys to clinical success with pulp capping: a review of the literature, Oper Dent, 34 (2009) 615–625. [PubMed: 19830978]

[4]. da Rosa WLO, Cocco AR, Silva TMD, Mesquita LC, Galarca AD, Silva AFD, Piva E, Current trends and future perspectives of dental pulp capping materials: A systematic review, J Biomed Mater Res B Appl Biomater, 106 (2018) 1358–1368. [PubMed: 28561919]

[5]. Reisine ST, Fertig J, Weber J, Leder S, Impact of dental conditions on patients'quality of life, Community Dentistry and Oral Epidemiology, 17 (1989) 7–10. [PubMed: 2645088]

[6]. Schwendicke F, Brouwer F, Schwendicke A, Paris S, Different materials for direct pulp capping: systematic review and meta-analysis and trial sequential analysis, Clinical Oral Investigations, 20 (2016) 1121–1132. [PubMed: 27037567]

[7]. Gronthos S, Mankani M, Brahim J, Robey PG, Shi S, Postnatal human dental pulp stem cells (DPSCs) in vitro and in vivo, Proceedings of the National Academy of Sciences, 97 (2000) 13625–13630.

[8]. Gronthos S, Brahim J, Li W, Fisher LW, Cherman N, Boyde A, DenBesten P, Robey PG, Shi S, Stem Cell Properties of Human Dental Pulp Stem Cells, Journal of Dental Research, 81 (2016) 531–535.

[9]. Mitsiadis TA, Orsini G, Jimenez-Rojo L, Stem cell-based approaches in dentistry, Eur Cell Mater, 30 (2015) 248–257. [PubMed: 26562631]

[10]. Tang Y, Wu X, Lei W, Pang L, Wan C, Shi Z, Zhao L, Nagy TR, Peng X, Hu J, Feng X, Van Hul W, Wan M, Cao X, TGF-beta1-induced migration of bone mesenchymal stem cells couples bone resorption with formation, Nat Med, 15 (2009) 757–765. [PubMed: 19584867]

[11]. Howard C, Murray PE, Namerow KN, Dental pulp stem cell migration, J Endod, 36 (2010) 1963–1966. [PubMed: 21092813]

[12]. Sadaghiani L, Gleeson HB, Youde S, Waddington RJ, Lynch CD, Sloan AJ, Growth Factor Liberation and DPSC Response Following Dentine Conditioning, J Dent Res, 95 (2016) 1298–1307. [PubMed: 27307049]

[13]. Okamoto M, Takahashi Y, Komichi S, Cooper PR, Hayashi M, Dentinogenic effects of extracted dentin matrix components digested with matrix metalloproteinases, Sci Rep, 8 (2018) 10690. [PubMed: 30013085]

[14]. Wang W, Dang M, Zhang Z, Hu J, Eyster TW, Ni L, Ma PX, Dentin regeneration by stem cells of apical papilla on injectable nanofibrous microspheres and stimulated by controlled BMP-2 release, Acta Biomater, 36 (2016) 63–72. [PubMed: 26971664]

[15]. Kuang R, Zhang Z, Jin X, Hu J, Gupte MJ, Ni L, Ma PX, Nanofibrous spongy microspheres enhance odontogenic differentiation of human dental pulp stem cells, Adv Healthc Mater, 4 (2015) 1993–2000. [PubMed: 26138254]

[16]. Kuang R, Zhang Z, Jin X, Hu J, Shi S, Ni L, Ma PX, Nanofibrous spongy microspheres for the delivery of hypoxia-primed human dental pulp stem cells to regenerate vascularized dental pulp, Acta Biomater, 33 (2016) 225–234. [PubMed: 26826529]

[17]. Johnstone RM, Adam M, Hammond JR, Orr L, Turbide C, Vesicle formation during reticulocyte maturation. Association of plasma membrane activities with released vesicles (exosomes), J Biol Chem, 262 (1987) 9412–9420. [PubMed: 3597417]

[18]. Tkach M, Thery C, Communication by Extracellular Vesicles: Where We Are and Where We Need to Go, Cell, 164 (2016) 1226–1232. [PubMed: 26967288]

[19]. Stanko P, Altanerova U, Jakubechova J, Repiska V, Altaner C, Dental Mesenchymal Stem/Stromal Cells and Their Exosomes, Stem Cells Int, 2018 (2018) 8973613. [PubMed: 29760738]

[20]. Fevrier B, Raposo G, Exosomes: endosomal-derived vesicles shipping extracellular messages, Curr Opin Cell Biol, 16 (2004) 415–421. [PubMed: 15261674]

[21]. Lener T, Gimona M, Aigner L, Borger V, Buzas E, Camussi G, Chaput N, Chatterjee D, Court FA, Del Portillo HA, O'Driscoll L, Fais S, Falcon-Perez JM, Felderhoff-Mueser U, Fraile L, Gho YS, Gorgens A, Gupta RC, Hendrix A, Hermann DM, Hill AF, Hochberg F, Horn PA, de Kleijn D, Kordelas L, Kramer BW, Kramer-Albers EM, Laner-Plamberger S, Laitinen S, Leonardi T, Lorenowicz MJ, Lim SK, Lotvall J, Maguire CA, Marcilla A, Nazarenko I, Ochiya T, Patel T, Pedersen S, Pocsfalvi G, Pluchino S, Quesenberry P, Reischl IG, Rivera FJ, Sanzenbacher R, Schallmoser K, Slaper-Cortenbach I, Strunk D, Tonn T, Vader P, van Balkom BW, Wauben M, Andaloussi SE, Thery C, Rohde E, Giebel B, Applying extracellular vesicles based therapeutics in clinical trials - an ISEV position paper, J Extracell Vesicles, 4 (2015) 30087. [PubMed: 26725829]

[22]. Galieva LR, James V, Mukhamedshina YO, Rizvanov AA, Therapeutic Potential of Extracellular Vesicles for the Treatment of Nerve Disorders, Front Neurosci, 13 (2019) 163. [PubMed: 30890911]

[23]. Connor DE, Paulus JA, Dabestani PJ, Thankam FK, Dilisio MF, Gross RM, Agrawal DK, Therapeutic potential of exosomes in rotator cuff tendon healing, J Bone Miner Metab, 37 (2019) 759–767. [PubMed: 31154535]

[24]. Ailawadi S, Wang X, Gu H, Fan G-C, Pathologic function and therapeutic potential of exosomes in cardiovascular disease, Biochimica et Biophysica Acta (BBA) - Molecular Basis of Disease, 1852 (2015) 1–11. [PubMed: 25463630]

[25]. Huang CC, Narayanan R, Alapati S, Ravindran S, Exosomes as biomimetic tools for stem cell differentiation: Applications in dental pulp tissue regeneration, Biomaterials, 111 (2016) 103–115. [PubMed: 27728810]

[26]. Hu X, Zhong Y, Kong Y, Chen Y, Feng J, Zheng J, Lineage-specific exosomes promote the odontogenic differentiation of human dental pulp stem cells (DPSCs) through TGFbeta1/smads signaling pathway via transfer of microRNAs, Stem Cell Res Ther, 10 (2019) 170. [PubMed: 31196201]

[27]. Li Y, Wang X, Ren J, Wu X, Li G, Fan Z, Zhang C, Li A, Wang S, Mandible exosomal ssc - mir-133b regulates tooth development in miniature swine via endogenous apoptosis, Bone Research, 6 (2018).

[28]. Jiang N, Xiang L, He L, Yang G, Zheng J, Wang C, Zhang Y, Wang S, Zhou Y, Sheu TJ, Wu J, Chen K, Coelho PG, Tovar NM, Kim SH, Chen M, Zhou YH, Mao JJ, Exosomes Mediate Epithelium-Mesenchyme Crosstalk in Organ Development, ACS Nano, 11 (2017) 7736–7746. [PubMed: 28727410]

[29]. Danhier F, Ansorena E, Silva JM, Coco R, Le Breton A, Préat V, PLGA-based nanoparticles: An overview of biomedical applications, Journal of Controlled Release, 161 (2012) 505–522. [PubMed: 22353619]

[30]. Wei G, Pettway GJ, McCauley LK, Ma PX, The release profiles and bioactivity of parathyroid hormone from poly(lactic-co-glycolic acid) microspheres, Biomaterials, 25 (2004) 345–352. [PubMed: 14585722]

[31]. Feng G, Zhang Z, Dang M, Zhang X, Doleyres Y, Song Y, Chen D, Ma PX, Injectable nanofibrous spongy microspheres for NR4A1 plasmid DNA transfection to reverse fibrotic degeneration and support disc regeneration, Biomaterials, 131 (2017) 86–97. [PubMed: 28376367]

[32]. Murillo-Martínez MM, Pedroza-Islas R, Lobato-Calleros C, Martínez-Ferez A, Vernon-Carter EJ, Designing W1/O/W2 double emulsions stabilized by protein–polysaccharide complexes for producing edible films: Rheological, mechanical and water vapour properties, Food Hydrocolloids, 25 (2011) 577–585.

[33]. Lin HP, Tu HP, Hsieh YP, Lee BS, Controlled release of lovastatin from poly(lactic-co-glycolic acid) nanoparticles for direct pulp capping in rat teeth, Int J Nanomedicine, 12 (2017) 5473–5485. [PubMed: 28814864]

[34]. Cvikl B, Hess SC, Miron RJ, Agis H, Bosshardt D, Attin T, Schmidlin PR, Lussi A, Response of human dental pulp cells to a silver-containing PLGA/TCP-nanofabric as a potential antibacterial regenerative pulp-capping material, BMC Oral Health, 17 (2017).

[35]. Zhao C, Tian S, Liu Q, Xiu K, Lei I, Wang Z, Ma PX, Biodegradable nanofibrous temperature-responsive gelling microspheres for heart regeneration, Advanced Functional Materials, 30 (2020).

[36]. Liu X, Ma PX, The nanofibrous architecture of poly(L-lactic acid)-based functional copolymers, Biomaterials, 31 (2010) 259–269. [PubMed: 19783035]

[37]. Zhang Z, Gupte MJ, Jin X, Ma PX, Injectable Peptide Decorated Functional Nanofibrous Hollow Microspheres to Direct Stem Cell Differentiation and Tissue Regeneration, Advanced Functional Materials, 25 (2015) 350–360. [PubMed: 26069467]

[38]. Zhang J, Liu X, Li H, Chen C, Hu B, Niu X, Li Q, Zhao B, Xie Z, Wang Y, Exosomes/tricalcium phosphate combination scaffolds can enhance bone regeneration by activating the PI3K/Akt signaling pathway, Stem Cell Res Ther, 7 (2016) 136. [PubMed: 27650895]

[39]. Jung KO, Jo H, Yu JH, Gambhir SS, Pratx G, Development and MPI tracking of novel hypoxia-targeted theranostic exosomes, Biomaterials, 177 (2018) 139–148. [PubMed: 29890363]

[40]. Rio DC, Ares M Jr., Hannon GJ, Nilsen TW, Purification of RNA using TRIzol (TRI reagent), Cold Spring Harb Protoc, 2010 (2010) pdb prot5439.

[41]. Livak KJ, Schmittgen TD, Analysis of relative gene expression data using real-time quantitative PCR and the 2(-Delta Delta C(T)) Method, Methods, 25 (2001) 402–408. [PubMed: 11846609]

[42]. Tang YT, Huang YY, Zheng L, Qin SH, Xu XP, An TX, Xu Y, Wu YS, Hu XM, Ping BH, Wang Q, Comparison of isolation methods of exosomes and exosomal RNA from cell culture medium and serum, Int J Mol Med, 40 (2017) 834–844. [PubMed: 28737826]

[43]. Wei G, Ma PX, Macroporous and nanofibrous polymer scaffolds and polymer/bone-like apatite composite scaffolds generated by sugar spheres, J Biomed Mater Res A, 78 (2006) 306–315. [PubMed: 16637043]

[44]. Gupte MJ, Swanson WB, Hu J, Jin X, Ma H, Zhang Z, Liu Z, Feng K, Feng G, Xiao G, Hatch N, Mishina Y, Ma PX, Pore size directs bone marrow stromal cell fate and tissue regeneration in nanofibrous macroporous scaffolds by mediating vascularization, Acta Biomater, 82 (2018) 1–11. [PubMed: 30321630]

[45]. Wei G, Jin Q, Giannobile WV, Ma PX, Nano-fibrous scaffold for controlled delivery of recombinant human PDGF-BB, J Control Release, 112 (2006) 103–110. [PubMed: 16516328]

[46]. Wei G, Jin Q, Giannobile WV, Ma PX, The enhancement of osteogenesis by nano-fibrous scaffolds incorporating rhBMP-7 nanospheres, Biomaterials, 28 (2007) 2087–2096. [PubMed: 17239946]

[47]. Dammaschke T, Rat molar teeth as a study model for direct pulp capping research in dentistry, Lab Anim, 44 (2010) 1–6. [PubMed: 19854755]

[48]. Marchesan J, Girnary MS, Jing L, Miao MZ, Zhang S, Sun L, Morelli T, Schoenfisch MH, Inohara N, Offenbacher S, Jiao Y, An experimental murine model to study periodontitis, Nat Protoc, 13 (2018) 2247–2267. [PubMed: 30218100]

[49]. van der Pol E, Hoekstra AG, Sturk A, Otto C, van Leeuwen TG, Nieuwland R, Optical and non-optical methods for detection and characterization of microparticles and exosomes, J Thromb Haemost, 8 (2010) 2596–2607. [PubMed: 20880256]

[50]. Bosch S, de Beaurepaire L, Allard M, Mosser M, Heichette C, Chrétien D, Jegou D, Bach J-M, Trehalose prevents aggregation of exosomes and cryodamage, Scientific Reports, 6 (2016).

[51]. Skalko-Basnet N, Biologics: the role of delivery systems in improved therapy, Biologics, 8 (2014) 107–114. [PubMed: 24672225]

[52]. Huang YJ, Chao SC, Lien DH, Wen CY, He JH, Lee SC, Dual-functional Memory and Threshold Resistive Switching Based on the Push-Pull Mechanism of Oxygen Ions, Sci Rep, 6 (2016) 23945. [PubMed: 27052322]

[53]. Akers JC, Ramakrishnan V, Yang I, Hua W, Mao Y, Carter BS, Chen CC, Optimizing preservation of extracellular vesicular miRNAs derived from clinical cerebrospinal fluid, Cancer Biomarkers, 17 (2016) 125–132. [PubMed: 27062568]

[54]. Pan Y, Li W, Wei NN, So YM, Lai X, Li Y, Jiang K, He G, Highly active rare-earth metal catalysts for heteroselective ring-opening polymerization of racemic lactide, Dalton Trans, 48 (2019) 9079–9088. [PubMed: 31017172]

[55]. Perez C, Castellanos IJ, Costantino HR, Al-Azzam W, Griebenow K, Recent trends in stabilizing protein structure upon encapsulation and release from bioerodible polymers, J Pharm Pharmacol, 54 (2002) 301–313. [PubMed: 11902796]

[56]. Cajazeira Aguiar M, Arana-Chavez VE, Ultrastructural and immunocytochemical analyses of osteopontin in reactionary and reparative dentine formed after extrusion of upper rat incisors, Journal of Anatomy, 210 (2007) 418–427. [PubMed: 17428203]

[57]. Cooper PR, Takahashi Y, Graham LW, Simon S, Imazato S, Smith AJ, Inflammation-regeneration interplay in the dentine-pulp complex, J Dent, 38 (2010) 687–697. [PubMed: 20580768]

[58]. Schroder U, Effects of calcium hydroxide-containing pulp-capping agents on pulp cell migration, proliferation, and differentiation, J Dent Res, 64 Spec No (1985) 541–548. [PubMed: 3857254]

[59]. Robbins PD, Morelli AE, Regulation of immune responses by extracellular vesicles, Nat Rev Immunol, 14 (2014) 195–208. [PubMed: 24566916]

[60]. Gimona M, Pachler K, Laner-Plamberger S, Schallmoser K, Rohde E, Manufacturing of Human Extracellular Vesicle-Based Therapeutics for Clinical Use, Int J Mol Sci, 18 (2017).

- Exosomes from dental pulp stem cells and odontoblast cells upregulate odontogenic genes
- Triblock copolymer is able to deliver exosomes with tunable dose and duration
- Sustained exosome release induces dental pulp stem cell migration and dentin regeneration
- Exosome-loaded dental pulp capping materials facilitate dentin bridge formation and protect pulp tissue

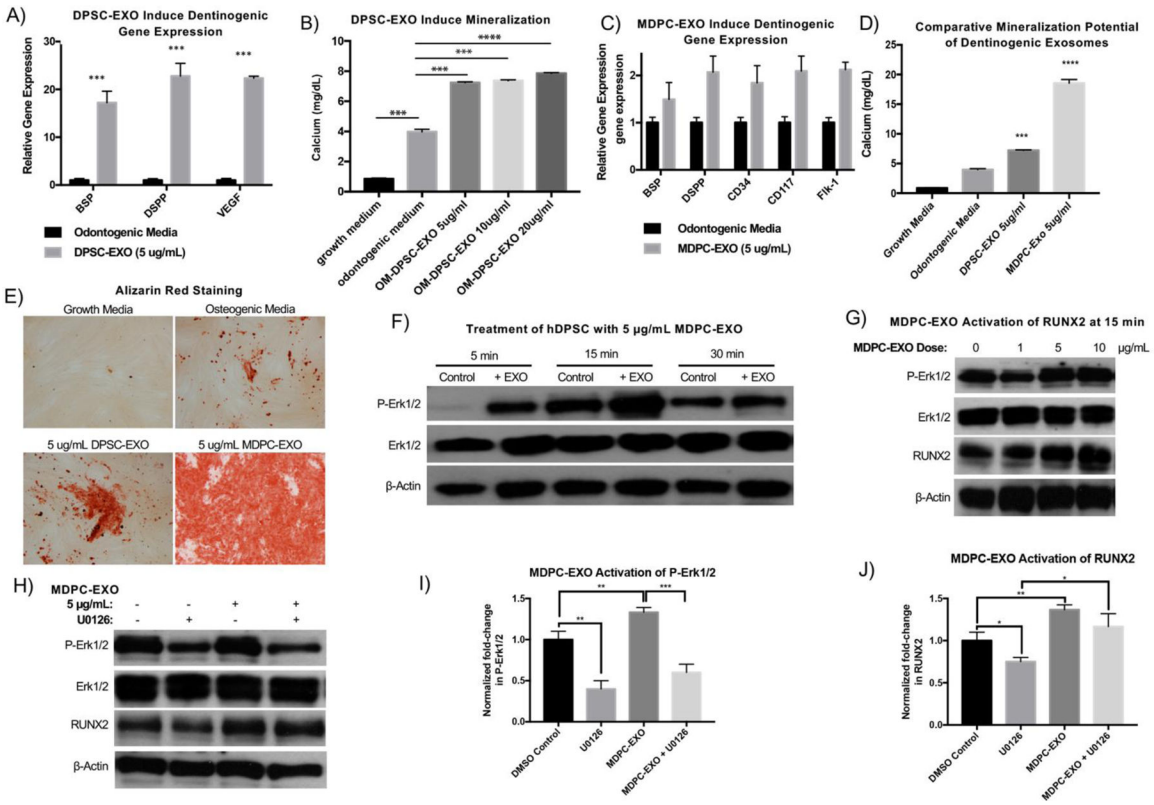

Figure 1.

hDPSCs were treated with DPSC-EXO (5 µg/mL) for one week, *in vitro*. Quantitative gene expression analysis demonstrates upregulation of genes characteristic of odontogenic differentiation in DPSC-EXO-treated hDPSCs, compared to untreated hDPSCs (A). Upregulated odontogenic gene expression corroborates with calcium mineral ization by treated and untreated hDPSCs over the course of two weeks, demonstrated by colorimetric assay (B). In the same fashion, hDPSCs were treated with MDPC-EXO (5 µg/mL) which showed similar characteristic upregulation in dentinogenic gene expression after 1 week (C). MDPC-EXO (5 µg/mL) induced significantly more mineralization after two weeks than DPSC-EXO, *in vitro*, measured by colorimetric assay (D) and visualized by alizarin red staining (E). To probe the mechanism by which MDPC-EXO upregulate the dentinogenic differentiation trajectory, Western blot analysis demonstrates increased Erk1/2 phosphorylation in a time-dependent (F) and dose-dependent (G) manner, which leads to upregulation of RUNX2 protein expression. Treatment with U0126, an inhibitor of MAPK signaling, was used to confirm the role of MAPK signaling in the MDPC-EXO-mediated upregulation of RUNX2 (H, I, J). * $p < 0.05$, ** $p < 0.01$, *** $p < 0.001$, **** $p < 0.0001$.

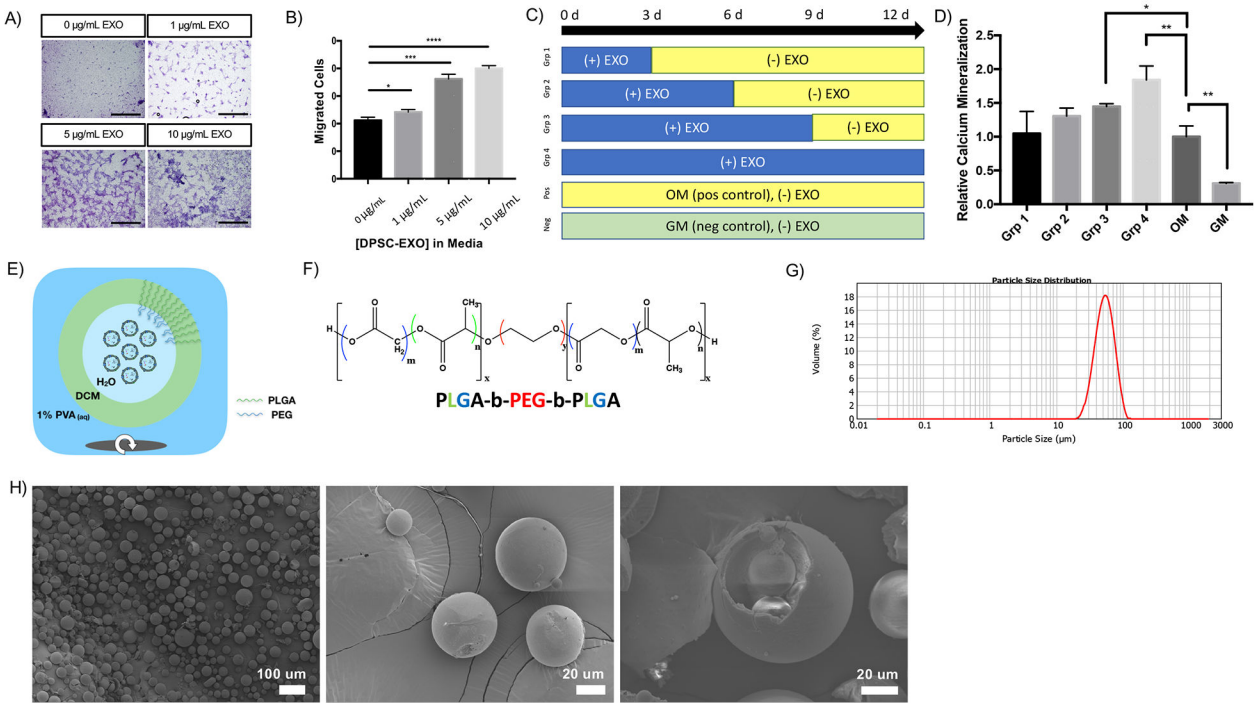

Figure 2.

In a transwell migration assay, DPSC-EXOs are shown to facilitate migration of nascent hDPSCs in a dose-dependent manner (A, scale = 200 µm, B). Prolonged exposure to DPSC-EXO in culture media results in increased mineralization, in a time-dependent manner where the duration of exposure correlates to the degree of mineralization by DPSCs, compared to odontogenic and growth media controls (C, D). The combination of these properties lends to the development of an *in vivo* delivery system for dentinogenic exosomes. Exosomes are encapsulated into polymeric microspheres by a double emulsion method (E). Exosomes, concentrated in PBS, are emulsified in a dichloromethane which contains PLGA-PEG-PLGA copolymer (F). The resulting emulsion is emulsified in 1% w/v polyvinyl alcohol to form discrete water-oil-water (w/o/w) droplets which contain exosomes in their inner water compartment. After solvent evaporation, resulting particles are collected and lyophilized. Their size is measured by Mastersizer laser diffraction (G, $d_{av\ g}$ = 51.885 µm) and particle morphology is assessed by scanning electron microscopy (H – left, scale = 100 µm; middle, scale = 20 µm; right, scale = 20 µm). * $p < 0.05$, ** $p < 0.01$, *** $p < 0.001$, **** $p < 0.0001$.

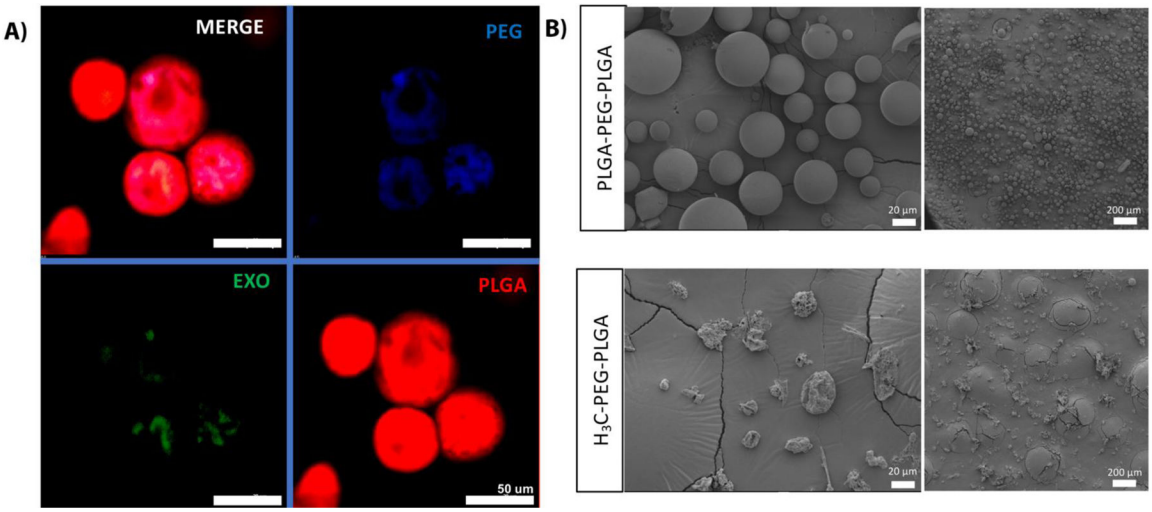

Figure 3.

Confocal microscopy is used to assess the self-assembling nature of PLGA-PEG-PLGA block copolymer in fabricating EXO-MS by fluorescently labelling copolymer segments (A, scale = 50 μm). PLGA (red, imaged with 561 nm laser channel) forms a uniform sphere, with pockets of interior PEG (blue, imaged with 405 nm laser channel) forming smaller spheres within the PLGA; fluorescently labelled exosomes (green, imaged with 488 nm laser channel) colocalize with PEG (blue) which facilitates encapsulation by self-assembly by forming hydrophilic pockets within the polymer MS. Compared to triblock PLGA-PEG-PLGA, diblock H_3C-PEG-PLGA results in less regularly shaped polymeric spheres. High magnification (B, left, scale = 20 μm) and low magnification (B, right, scale = 200 μm).

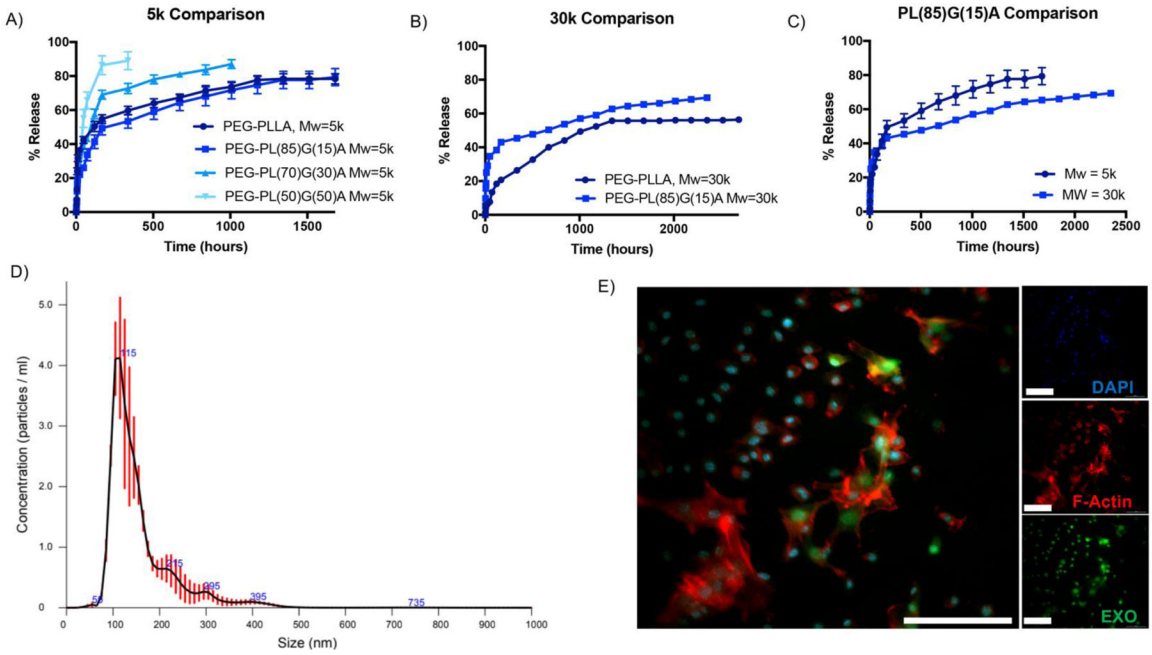

Figure 4.

Exosomes are released from EXO-MS when incubated *in vitro*. The release profile is a function of molecular weight and hydrophilicity of the PLGA-PEG-PLGA copolymers (A, B, C). Released exosomes maintain their characteristic hydrodynamic diameter and size distribution at 1-week time point (D), indicating that the lipid membrane remains intact and undisrupted throughout encapsulation and release. DiO-labelled exosomes were encapsulated and released from the EXO-MS, and their rapid uptake into the cytoplasm of recipient hDPSCs was visualized by confocal microscopy (E, 30 minutes incubation. Blue = DAPI, Red = F-actin, Green = DPSC-EXO, scale = 100 μm).

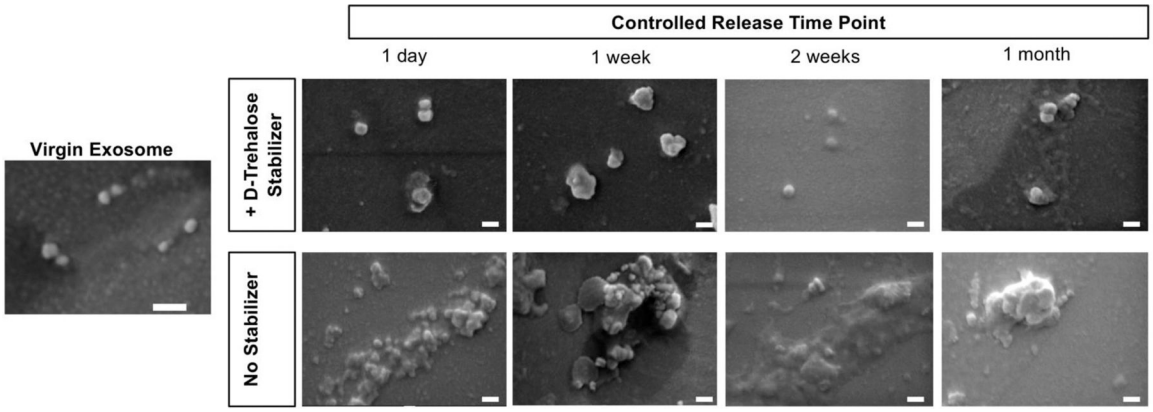

Figure 5.

D-Trehalose, a hydrophilic disaccharide, is used as a stabilizer to protect exosomes and prevent aggregation during encapsulation and release. Scanning electron microscopy evaluation of exosome morphology indicates that throughout various release time points, the inclusion of D-trehalose (2 mM) minimizes aggregate size of exosomes, leading to a more uniform release from the polymer microspheres, compared to those encapsulated without the addition of D-trehalose (scale = 100 nm).

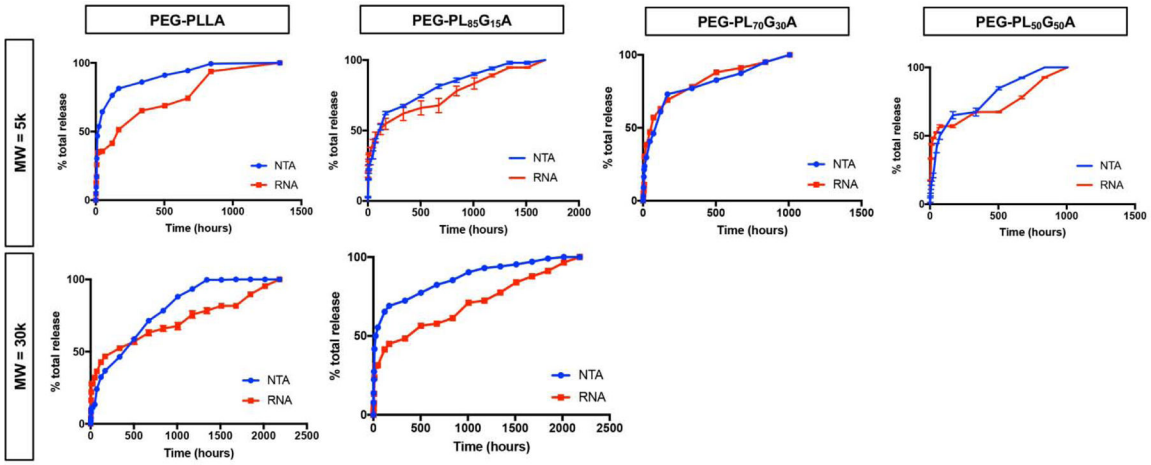

Figure 6.

Quantification of the release profile of exosomes from EXO-MS polymer spheres over time. Particle number, assessed by nanotracking analysis (blue), corroborates well with the amount of RNA isolated from each release aliquot (red), indicating that exosome cargo is preserved throughout encapsulation and release.

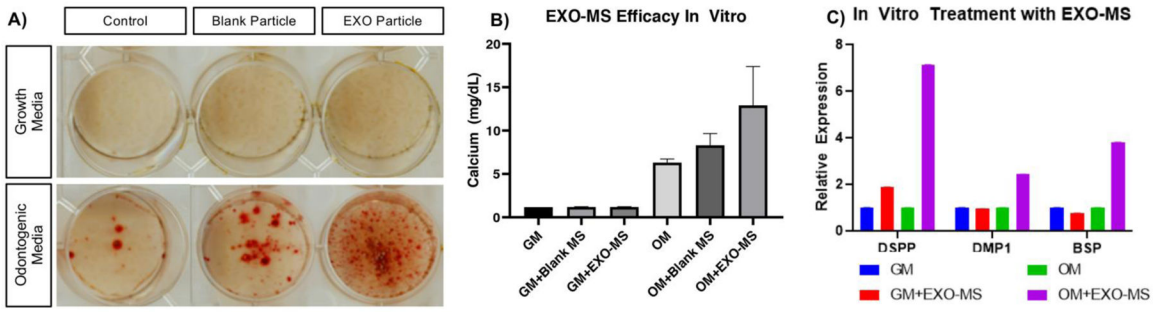

Figure 7.

DPSC-EXO were used as cargo to validate the EXO-MS platform *in vitro*. Biologic activity of EXO-MS eluent (0.1 mg/mL EXO-MS in odontogenic media) demonstrated by mineralization (A, B) and odontogenic differentiation (C) of hDPSCs after two weeks of exposure, due to the controlled release of DPSC-EXO. Blank EXO-MS showed negligible therapeutic effect, while DPSC-EXO loaded EXO-MS showed significant increases in both mineralization and odontogenic gene expression.

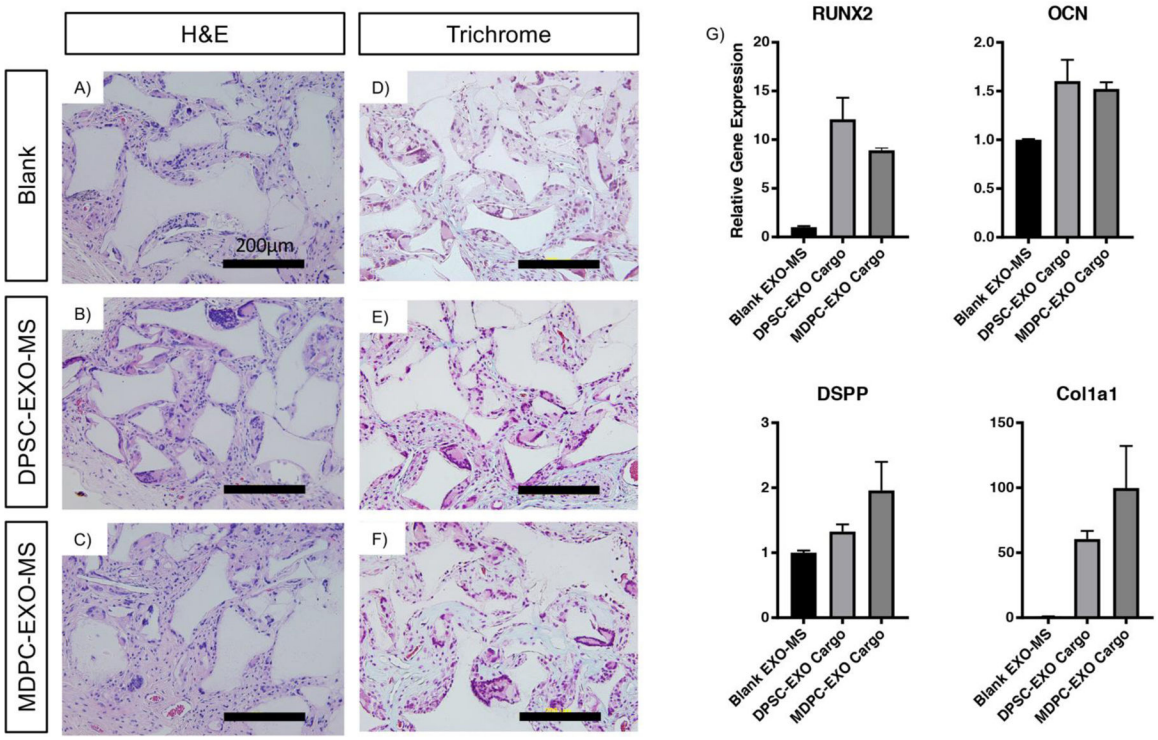

Figure 8.

Subcutaneous implantation of EXO-MS constructs. Compared to blank EXO-MS, DPSC-EXO-MS and MDPC-EXO-MS constructs seeded with mDPSCs showed increased cellularity by hematoxylin and eosin staining (A, B, C), and more intense Masson's Trichrome staining indicative of increased collagen expression (D, E, F). Gene expression data (G) indicates that the controlled release of both DPSC-EXO and MDPC-EXO from EXO-MS enhances significant DPSC differentiation towards an odontogenic phenotype (Scale = 200 um).

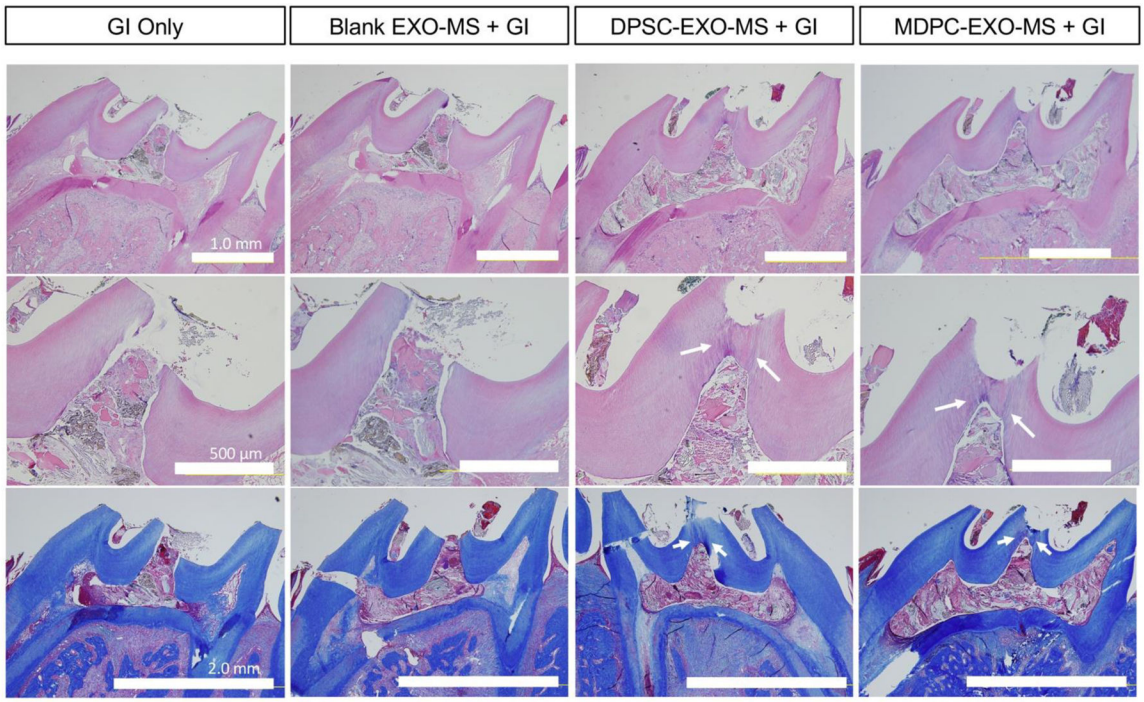

Figure 9.

EXO-MS as a biomimetic pulp capping agent, evaluated *in vivo* in a rat pulp-capping model. Top row (H&E), Mag: 4x, Scale: 1.0 mm; Middle row (H&E), Mag: 10x, scale: 500 µm; Bottom row (Trichrome), Mag: 4x, scale: 2.0 mm. Arrows point to the margin of reactionary dentin formation.